



HAL
open science

Fast Gradient-Free Optimization in Distributed Multi-User MIMO Systems

Olivier Bilenne, Panayotis Mertikopoulos, Elena Veronica Belmega

► **To cite this version:**

Olivier Bilenne, Panayotis Mertikopoulos, Elena Veronica Belmega. Fast Gradient-Free Optimization in Distributed Multi-User MIMO Systems. 2020. hal-02861460v1

HAL Id: hal-02861460

<https://hal.science/hal-02861460v1>

Preprint submitted on 9 Jun 2020 (v1), last revised 23 Oct 2020 (v2)

HAL is a multi-disciplinary open access archive for the deposit and dissemination of scientific research documents, whether they are published or not. The documents may come from teaching and research institutions in France or abroad, or from public or private research centers.

L'archive ouverte pluridisciplinaire **HAL**, est destinée au dépôt et à la diffusion de documents scientifiques de niveau recherche, publiés ou non, émanant des établissements d'enseignement et de recherche français ou étrangers, des laboratoires publics ou privés.

Fast Gradient-Free Optimization in Distributed Multi-User MIMO Systems

Olivier Bilenne, Panayotis Mertikopoulos, *Member, IEEE* and E. Veronica Belmega, *Senior Member, IEEE*

Abstract—In this paper, we develop a gradient-free optimization methodology for efficient resource allocation in Gaussian MIMO multiple access channels. Our approach combines two main ingredients: (i) the entropic semidefinite optimization method of matrix exponential learning (MXL); and (ii) a one-shot gradient estimator which achieves low variance through the reuse of past information. Owing to this reuse mechanism, the proposed *gradient-free MXL algorithm with callbacks* (MXL0⁺) retains the convergence speed of gradient-based methods while requiring minimal feedback per iteration—a *single scalar*. In more detail, in a MIMO multiple access channel with K users and M transmit antennas per user, the MXL0⁺ algorithm achieves ε -optimality within $\text{poly}(K, M)/\varepsilon^2$ iterations (on average and with high probability), even when implemented in a fully distributed, asynchronous manner. For cross-validation, we also perform a series of numerical experiments in medium- to large-scale MIMO networks under realistic channel conditions. Throughout our experiments, the performance of MXL0⁺ matches—and sometimes exceeds—that of gradient-based MXL methods, all the while operating with a vastly reduced communication overhead. In view of these findings, the MXL0⁺ algorithm appears to be uniquely suited for distributed massive MIMO systems where gradient calculations can become prohibitively expensive.

Index Terms—Gradient-free optimization; matrix exponential learning; multi-user MIMO networks; throughput maximization.

I. INTRODUCTION

THE deployment of multiple-input and multiple-output (MIMO) terminals at a massive scale has been identified as one of the key enabling technologies for fifth generation (5G) wireless networks, and for good reason: mass-MIMO arrays can increase throughput by a factor of $10\times$ to $100\times$ (or more), they improve the system’s robustness to ambient noise and channel fluctuations, and they bring about significant latency reductions over the air interface [1, 2]. Moreover, ongoing discussions for the evolution of 5G envision the deployment of advanced MIMO technologies at an even larger scale in order to reach the throughput and spectral efficiency required for “speed of thought” connectivity [3, 4].

In view of this, there have been intense efforts to meet the complex technological requirements that the mass-MIMO paradigm entails. At the hardware level, this requires scaling up existing multiple-antenna transceivers through the use of inexpensive service antennas and/or time-division duplexing (TDD)

[1, 5, 6]. At the same time however, given the vast amount of resources involved in upgrading an ageing infrastructure, a brute-force approach based solely on the evolution of wireless hardware technology cannot suffice. Instead, unleashing the full potential of mass-MIMO arrays requires a principled approach with the aim of minimizing computational overhead and related expenditures as the network scales up to accommodate more and more users.

In this general multi-user MIMO context, it is crucial to optimize the input signal covariance matrix of each user, especially in the moderate (or low) signal to interference-plus-noise ratio (SINR) regime [7–11]. The conventional approach to this problem involves the use of water-filling (WF) solution methods, either iterative [8, 12] or simultaneous [13]. However, such schemes invariably rely on the availability of perfect channel state information at the transmitter (CSIT), and are highly susceptible to observation noise, asynchronicities, and other impediments that arise in the presence of situational uncertainty. As a result, traditional water-filling approaches cannot be readily applied in real-world MIMO systems, especially when faced with the operational “fog of war” of distributed systems.

An appealing alternative to water-filling was recently proposed by the authors of [14] who introduce a semidefinite optimization method based on *matrix exponential learning* (MXL). The MXL algorithm proceeds incrementally by combining (stochastic) gradient steps with a matrix exponential mapping that ensures feasibility of the users’ signal covariance variables. In so doing, MXL guarantees fast convergence in cases where WF methods demonstrably fail: specifically, MXL achieves ε -optimality within $\mathcal{O}(1/\varepsilon^2)$ iterations, even in the presence of noisy gradient observations and/or asynchronous user updates.

On the negative side, MXL requires (i) inverting a relatively large matrix at the receiver; and, subsequently, (ii) broadcasting the resulting (dense) matrix to all connected users.¹ In a MIMO array with $N = 128$ receive antennas, this would correspond to transmitting approximately 65 kB of data per frame, thus exceeding typical frame size limitations by a factor of $50\times$ to $500\times$ (depending on the specific standard in use) [15]. Coupled with the significant energy expenditures involved in matrix computations and the fact that entry-level antenna arrays may be ill-equipped for this purpose, the computational overhead of MXL (or any other gradient-based method) quickly becomes prohibitive as MIMO systems “go large”. As a result, real-world MIMO networks are typically called to operate with minimal information at the receiver end, often limited to observations of

O. Bilenne and P. Mertikopoulos are with Univ. Grenoble Alpes, CNRS, Inria, Grenoble INP, LIG, 38000 Grenoble, France. E. V. Belmega is with ETIS UMR8051, CY University, ENSEA, CNRS, F-95000, Cergy, France.

The authors are grateful for financial support from the French National Research Agency (ANR) projects ORACLESS (ANR-16-CE33-0004-01) and ELIOT (ANR-18-CE40-0030 and FAPESP 2018/12579-7). The research of P. Mertikopoulos has also received financial support from the COST Action CA 16228 ‘European Network for Game Theory’ (GAMENET).

¹Water-filling methods have the same exact requirement, so this issue cannot be circumvented by reverting to a WF-based scheme.

the achieved throughput.

Contributions and related work: Our main objective in this paper is to overcome the above limitations by working in a “gradient-free” framework, i.e., by lifting the vital assumption that the network’s users have access to gradient information. For concreteness, we focus on the problem of throughput maximization in Gaussian MIMO multiple access channels (MACs), and we construct a one-shot gradient estimator from achieved throughput information using a technique known as *simultaneous perturbation stochastic approximation* (SPSA) [16, 17]. By integrating this SPSA estimator in the chassis of the MXL method, we obtain a *gradient-free matrix exponential learning* (MXL0), which we show converges to ε -optimality within $\mathcal{O}(1/\varepsilon^4)$ iterations (on average and with high probability).²

Despite the vastly reduced computational overhead of the zeroth-order MXL0 method, the drop in convergence speed relative to the original MXL scheme is substantial and makes the algorithm ill-suited for practical systems. In fact, as we show via numerical experiments in realistic network conditions, MXL0 might take up to 10^5 iterations to achieve a relative optimality threshold of $\varepsilon = 10^{-1}$ (compared to around 10^2 iterations for MXL). This is caused by the very high variance of the SPSA estimator which incurs a significant amount of state space exploration and results in a drastic drop in the the algorithm’s convergence speed hitting nonviable levels.

To circumvent this obstacle, we introduce an effective variance reduction mechanism where previous information is reused to improve the accuracy of the SPSA gradient estimator. In this way, the resulting *gradient-free MXL algorithm with callbacks* (MXL0⁺) combines the best of both worlds: it retains the fast $\mathcal{O}(1/\varepsilon^2)$ convergence rate of the standard MXL algorithm, despite the fact that it only requires a *single scalar* worth of feedback per iteration. Quite remarkably, in many instances, the reuse of past queries turns out to be so efficient that the gradient-free MXL0⁺ algorithm outperforms even the original MXL method.

To the best of our knowledge, the work which is closest in spirit to our own is the very recent paper [18], where the authors seek to minimize the informational exchange of MXL methods applied to the maximization of transmit energy efficiency (as opposed to throughput). Specifically, instead of broadcasting an $N \times N$ Hermitian matrix, each receiver is assumed to transmit a random selection of components of the gradient for all connected users. This (batch) “coordinate descent” approach leads to an interesting tradeoff between signalling overhead and speed of convergence, but still relies on users having access to first-order gradient information. By contrast, we do not make any such assumption and work solely with throughput observations; in this way, the communication overhead is reduced to broadcasts of a single scalar, while retaining the possibility of asynchronous, distributed updates.

Paper outline: After presenting our system model in Section II and the original MXL method, we introduce in Section III the MXL0 algorithm based on SPSA gradient estimates. Subsequently, to bridge the gap between the slow

convergence of MXL0 relative to MXL, we introduce in Section IV a callback mechanism which allows us to derive a one-shot gradient estimator with drastically reduced variance. Our theoretical results for MXL0⁺ are presented in Section IV, while its asynchronous, distributed variants are discussed in Section V. Finally, our theoretical analysis is supplemented and validated with a series of numerical experiments in Section VI.

Notation: Throughout the sequel, we use bold capital letters for matrices, saving the letters k, ℓ for user assignments and t, s for time indices, so that e.g., matrix \mathbf{Q}_k relates to user k , \mathbf{Q}_t to time t , and $\mathbf{Q}_{k,t}$ to user k at time t . The symbols $o(\cdot)$, $\mathcal{O}(\cdot)$, and $\Theta(\cdot)$ are taken as in the common Bachmann-Landau notation.

II. PROBLEM STATEMENT

A. Problem setup and preliminaries

Consider a Gaussian vector multiple access channel consisting of K users simultaneously transmitting to a wireless receiver equipped with N antennas. If the k -th transmitter is equipped with M_k antennas, we get the baseband signal model

$$\mathbf{y} = \sum_{k=1}^K \mathbf{H}_k \mathbf{x}_k + \mathbf{z}, \quad (1)$$

where: a) $\mathbf{x}_k \in \mathbb{C}^{M_k}$ denotes the signal transmitted by the k -th user; b) $\mathbf{H}_k \in \mathbb{C}^{N \times M_k}$ is the corresponding channel matrix; c) $\mathbf{y} \in \mathbb{C}^N$ is the aggregate signal reaching the receiver; and d) $\mathbf{z} \in \mathbb{C}^N$ denotes the ambient noise in the channel, including thermal and environmental interference effects (and modeled for simplicity as a zero-mean, circulant Gaussian vector with unit covariance). In this general model, the transmit power of the k -th user is given by $p_k = \mathbb{E}[\mathbf{x}_k^\dagger \mathbf{x}_k]$. Then, letting P_k denote the maximum transmit power of user k , we also write

$$\mathbf{Q}_k = \mathbb{E}[\mathbf{x}_k \mathbf{x}_k^\dagger] / P_k \quad (2)$$

for the normalized signal covariance matrix of user k . By definition, \mathbf{Q}_k is Hermitian and positive-semidefinite, which we denote by writing $\mathbf{Q}_k \in \text{Herm}(M_k)$ and $\mathbf{Q}_k \succcurlyeq 0$ respectively.

Assuming that messages are decoded using successive interference cancellation (SIC) at the receiver, the users’ achievable sum rate is given by the familiar expression [19]:

$$R(\mathbf{Q}) = \log \det \left(\mathbf{I} + \sum_{k=1}^K P_k \mathbf{H}_k \mathbf{Q}_k \mathbf{H}_k^\dagger \right) \quad (3)$$

where $\mathbf{Q} \equiv (\mathbf{Q}_1, \dots, \mathbf{Q}_K)$ denotes the users’ aggregate signal covariance profile. Since $R(\mathbf{Q})$ is increasing in each user’s total transmit power $p_k = P_k \text{tr}(\mathbf{Q}_k)$, the channel’s throughput is maximized when the users individually saturate their power, i.e., when $\text{tr}(\mathbf{Q}_k) = 1$ for all $k = 1, \dots, K$. We thus obtain the *sum-rate optimization problem*

$$\begin{aligned} & \text{maximize} && R(\mathbf{Q}) \equiv R(\mathbf{Q}_1, \dots, \mathbf{Q}_K) \\ & \text{subject to} && \mathbf{Q}_k \in \mathcal{Q}_k \text{ for all } k = 1, \dots, K, \end{aligned} \quad (\text{Opt})$$

where each user’s feasible power region \mathcal{Q}_k is given by

$$\mathcal{Q}_k = \{\mathbf{Q}_k \in \text{Herm}(M_k) : \text{tr}(\mathbf{Q}_k) = 1, \mathbf{Q}_k \succcurlyeq 0\}. \quad (4)$$

²The “0” in our naming scheme refers to the fact that the algorithm requires only *zeroth-order* feedback—i.e., no first-order derivatives of R .

By definition, each \mathcal{Q}_k is a spectrahedron of (real) dimension $d_k = M_k^2 - 1$, so the problem's dimensionality is $\sum_k d_k = \mathcal{O}(\sum_k M_k^2)$. To avoid trivialities, we will assume in what follows that each transmitter possesses at least two antennas, so $d_k > 0$ for all $k = 1, \dots, K$. Also, to further streamline our discussion, we will state our results in terms of the maximum number $M = \max_k M_k$ of antennas per transmitter—or, equivalently, in terms of the larger dimension $d = M^2 - 1$.³

Alternatively, if messages are decoded using single user decoding (SUD) at the receiver (i.e., interference by non-focal users is treated as additive colored noise), each user's *individual* rate will be

$$R_k(\mathbf{Q}_k; \mathbf{Q}_{-k}) = R(\mathbf{Q}_1, \dots, \mathbf{Q}_K) - R(\mathbf{Q}_1, \dots, 0, \dots, \mathbf{Q}_K), \quad (5)$$

where $(\mathbf{Q}_k; \mathbf{Q}_{-k})$ is shorthand for $(\mathbf{Q}_1, \dots, \mathbf{Q}_k, \dots, \mathbf{Q}_K)$. In turn, this leads to the *individual* rate maximization problem

$$\begin{aligned} & \text{maximize} && R_k(\mathbf{Q}_k; \mathbf{Q}_{-k}) \\ & \text{subject to} && \mathbf{Q}_k \in \mathcal{Q}_k \end{aligned} \quad (\text{Opt}_k)$$

to be solved concurrently by each user $k = 1, \dots, K$. Given that $R(\mathbf{Q})$ is concave in \mathbf{Q} and $R_k(\mathbf{Q}_k; \mathbf{Q}_{-k})$ is concave in \mathbf{Q}_k , it follows that (Opt_k) defines a concave potential game whose Nash equilibria coincide with the solutions of (Opt) [14, 20, 21]. In view of this, (Opt) is amenable to a distributed approach where it is treated as the agglomeration of the unilateral sub-problems (Opt_k) , to be solved in parallel by the network's users. We revisit this distributed approach in Section V.

B. Matrix exponential learning (MXL)

The baseline solution method for (Opt) is the water-filling (WF) algorithm [7, 8, 22] and its variants—iterative or simultaneous [12, 13, 23]. In WF schemes, transmitters are tacitly assumed to have full knowledge of the channel as well as the signal covariance matrices of other users via the multi-user interference-plus-noise (MUI) covariance matrices

$$\mathbf{W}_k = \mathbf{I} + \sum_{\ell \neq k} \mathbf{H}_\ell \mathbf{Q}_\ell \mathbf{H}_\ell^\dagger \quad (6)$$

which are then used to “water-fill” the users' effective channel matrices $\tilde{\mathbf{H}}_k = \mathbf{W}_k^{-1/2} \mathbf{H}_k$. This is done either iteratively (in a round-robin fashion) or simultaneously (all transmitters at the same time); the former scheme converges always (but slowly if the number of users is large), whereas the latter may fail to converge altogether [13, 24]. In addition, WF is highly susceptible to observation noise, asynchronicities, and other impediments that arise in real-world systems, so the solution of (Opt) in a distributed, online manner requires different techniques.

These robustness limitations can be overcome via the use of first-order methods that are provably resilient to noise and other situational uncertainty impediments. This observation was the guiding principle behind the *matrix exponential learning* (MXL) algorithm [14, 25], which will serve both as reference and as an entry point for our analysis.

³The statement of our results can be finetuned at the cost of introducing further notation for other aggregate statistics of the number of antennas per transmitter (such as the arithmetic or geometric mean of M_k). The resulting expressions are fairly cumbersome, so we do not report them here.

To state it, let

$$\nabla_k R(\mathbf{Q}) = P_k \mathbf{H}_k^\dagger \left[\mathbf{I} + \sum_{\ell=1}^K P_\ell \mathbf{H}_\ell \mathbf{Q}_\ell \mathbf{H}_\ell^\dagger \right]^{-1} \mathbf{H}_k. \quad (7)$$

denote the individual gradient of R relative to the signal covariance matrix of the k -th user, and let

$$\mathcal{Y}_k = \{\mathbf{Y}_k \in \text{Herm}(M_k) : \text{tr}(\mathbf{Y}_k) = 0\} \quad (8)$$

denote the subspace tangent to \mathcal{Q} . Then, given an initial “score matrix” $\mathbf{Y}_1 \in \mathcal{Y} \equiv \prod_k \mathcal{Y}_k$, the MXL algorithm is defined via the basic recursion

$$\begin{aligned} \mathbf{Q}_t &= \Lambda(\mathbf{Y}_t), \\ \mathbf{Y}_{t+1} &= \mathbf{Y}_t + \gamma_t \mathbf{V}_t, \end{aligned} \quad (\text{MXL})$$

where:

- a) \mathbf{Q}_t denotes the users' input signal covariance profile at the t -th iteration of the algorithm ($t = 1, 2, \dots$).
- b) $\mathbf{V}_t = (\mathbf{V}_{1,t}, \dots, \mathbf{V}_{K,t})$ is an estimate of the tangent component of the gradient ∇R relative to \mathcal{Q} .⁴
- c) $\gamma_t > 0$ is a non-increasing sequence of step-sizes whose role is examined in detail below.
- d) \mathbf{Y}_t is an auxiliary matrix that aggregates gradient steps.
- e) $\Lambda(\mathbf{Y}) = (\Lambda_1(\mathbf{Y}_1), \dots, \Lambda_K(\mathbf{Y}_K))$ denotes the matrix exponential mapping given in (block) components by

$$\Lambda_k(\mathbf{Y}_k) = \frac{\exp(\mathbf{Y}_k)}{\text{tr}(\exp(\mathbf{Y}_k))}. \quad (9)$$

The intuition behind (MXL) is that the exponential mapping assigns more power to the spatial directions that are aligned to the objective's gradient (as estimated via \mathbf{V}_t). In fact, the MXL algorithm can be explained as a matrix-valued instance of Nesterov's dual averaging method [26] with entropic regularization; we defer the details of this derivation to Appendix A.

As was shown in [14], the MXL algorithm achieves an ε -optimal signal covariance profile within $\mathcal{O}(1/\varepsilon^2)$ iterations. However, to do so, the algorithm still requires access to noisy observations of the gradient matrices (7). Typically, this involves inverting a (dense) $N \times N$ Hermitian matrix at a central hub and subsequently broadcasting the result, so the algorithm's computation and communication overhead remains significant. Also, it is not clear how the method could be implemented in a fully distributed setting. On that account, our main focus in the sequel will be to lift the assumption that the network's users have access to the gradient matrices (7), all the while maintaining the $\mathcal{O}(1/\varepsilon^2)$ convergence speed of (MXL).

C. Technical preliminaries and notation

For the analysis to come, it will be convenient to introduce the following constants. First, we will write $\mathcal{Q} = \prod_k \mathcal{Q}_k$ for the feasible region of (Opt) , and we will denote by L the Lipschitz constant of R over \mathcal{Q} relative to the nuclear norm; specifically, this means that:

$$|R(\mathbf{Q}) - R(\mathbf{Q}')| \leq L \|\mathbf{Q} - \mathbf{Q}'\| \quad \text{for all } \mathbf{Q}, \mathbf{Q}' \in \mathcal{Q}. \quad (10)$$

⁴More precisely, (MXL) only requires estimates of $\nabla R : \mathcal{Q} \mapsto \mathcal{Y}$, which here denotes the tangent component of the gradient ∇R relative to \mathcal{Q} , given by $\nabla R = (\nabla_1 R, \dots, \nabla_K R)$ where $\nabla_k R = \nabla_k R - \text{tr}(\nabla_k R) \mathbf{I}$. All technical details in regards to (MXL) are deferred to the appendix.

Moreover, we will also write $\lambda_{k\ell}$ for the user-specific Lipschitz constants of $\nabla_k R$, understood in the following sense:

$$\|\nabla_k R(\mathbf{Q}_\ell; \mathbf{Q}_{-\ell}) - \nabla_k R(\mathbf{Q}'_\ell; \mathbf{Q}_{-\ell})\|_* \leq \lambda_{k\ell} \|\mathbf{Q}_\ell - \mathbf{Q}'_\ell\|_2, \quad (11)$$

for all $\mathbf{Q}_\ell, \mathbf{Q}'_\ell \in \mathcal{Q}_\ell$, $\mathbf{Q}_{-\ell} \in \mathcal{Q}_{-\ell} \equiv \prod_{j \neq \ell} \mathcal{Q}_j$, and all $k, \ell = 1, \dots, K$. We also let $\lambda_k = (1/K) \sum_{\ell=1}^K \lambda_{k\ell}$ denote the ‘‘averaged’’ Lipschitz constant of user k , and we write $\lambda = (1/K) \sum_{k=1}^K \lambda_k$ for the overall ‘‘mean’’ Lipschitz constant. For a detailed discussion of the nuclear norm $\|\cdot\|_*$ and its dual $\|\cdot\|_2$, we refer the reader to Appendix A.

III. MXL WITHOUT GRADIENT INFORMATION

As we noted above, the existing implementations of MXL invariably rely on the availability of gradient feedback—full [25], noisy [14], or partial [18]. Our aim in this section is to show that this need can be obviated by means of a (possibly biased) gradient estimator which only requires observations of a *single* scalar—the users’ achieved throughput.

A. Simultaneous perturbation stochastic approximation

Our approach builds on the method of *simultaneous perturbation stochastic approximation* (SPSA), a gradient estimation procedure which has become the cornerstone of large-scale, derivative-free optimization [16, 17]. To develop some intuition for the method, consider a differentiable function $f : \mathbb{R} \mapsto \mathbb{R}$. Then, by definition, the derivative of f at any point x satisfies

$$f'(x) = \frac{f(x+\delta) - f(x-\delta)}{2\delta} + o(\delta). \quad (12)$$

Therefore, if $\delta > 0$ is small enough, an estimate for $f'(x)$ can be obtained from two queries of the value of f at the neighboring points $x - \delta$ and $x + \delta$ as follows:

$$\hat{v}(x) = \frac{f(x+\delta) - f(x-\delta)}{2\delta}. \quad (13)$$

Thus, if f' is λ -Lipschitz continuous on the search domain, it is easy to see that the error of the estimator $\hat{v}(x)$ is uniformly bounded as $|\hat{v}(x) - f'(x)| \leq \lambda\delta/2$, i.e., the estimator (13) is accurate up to $\mathcal{O}(\delta)$.

Taking this idea further, it is possible to estimate $f'(x)$ using only a *single* function query at either of the test points $x - \delta$, or $x + \delta$, chosen randomly. To carry this out, let z be a random variable taking the value -1 or $+1$ with equal probability $1/2$, and define the *one-shot* SPSA estimator

$$v(x) = \frac{f(x + \delta z)}{\delta} z. \quad (14)$$

Then, a straightforward calculation gives $\mathbb{E}[v(x)] = \hat{v}(x)$, i.e., v is a stochastic estimator of f' with accuracy

$$|\mathbb{E}[v(x)] - f'(x)| = |\hat{v}(x) - f'(x)| \leq \lambda\delta/2 = \mathcal{O}(\delta). \quad (15)$$

The SPSA approach described above can be applied to our MIMO setting as follows. First, each user k draws, randomly and independently, a matrix \mathbf{Z}_k from the unit sphere⁵

$$\mathbf{S}^{d_k-1} = \{\mathbf{Z}_k \in \mathcal{Y}_k : \|\mathbf{Z}_k\|_2 = 1\}. \quad (16)$$

⁵Note that the dimension of \mathbf{S}^{d_k-1} as a manifold is $d_k - 1$, i.e., one lower than that of the feasible region \mathcal{Q}_k ; this is due to the unit norm constraint $\|\mathbf{Z}_k\|_2 = 1$.

Then, translating (14) to the distributed, Hermitian setting of Section II yields, for all $k = 1, \dots, K$, the gradient estimator

$$\mathbf{V}_k(\mathbf{Q}) = \frac{d_k}{\delta} R(\mathbf{Q} + \delta \mathbf{Z}) \mathbf{Z}_k, \quad (17)$$

where $\mathbf{Z} = (\mathbf{Z}_1, \dots, \mathbf{Z}_K)$ collects the random shifts of all users.

Remark 1. The factor $d_k = M_k^2 - 1$ in (17) has a geometric interpretation as the ratio between the volumes of the sphere \mathbf{S}^{d_k-1} (where \mathbf{Z}_k is drawn from) and the containing d_k -dimensional ball $\mathbb{B}^{d_k} = \{\mathbf{Z}_k \in \mathcal{Y}_k : \|\mathbf{Z}_k\|_2 \leq 1\}$. Its presence is due to Stokes’ theorem, as detailed in Lemma B.1.

A further complication that arises in our constrained setting is that the query point $\mathbf{Q} + \delta \mathbf{Z}$ in (17) may lie outside the feasible set \mathcal{Q} if \mathbf{Q} is too close to the boundary of \mathcal{Q} . To avoid such an occurrence, we introduce below a ‘‘safety net’’ mechanism which systematically carries back the pivot points \mathbf{Q}_k towards the ‘‘prox-center’’ $\mathbf{C}_k = \mathbf{I}_{M_k}/M_k$ of \mathcal{Q}_k before applying the random shift \mathbf{Z}_k . Specifically, taking $r_k > 0$ sufficiently small so that the Frobenius ball centered at \mathbf{C}_k lies entirely in \mathcal{Q}_k , we consider the homothetic adjustment

$$\hat{\mathbf{Q}}_k = \mathbf{Q}_k + \frac{\delta}{r_k} (\mathbf{C}_k - \mathbf{Q}_k) + \delta \mathbf{Z}_k. \quad (18)$$

By an elementary geometric argument, it suffices to take

$$r_k = 1/\sqrt{M_k(M_k - 1)}. \quad (19)$$

With this choice of r_k , it is easy to show that, for $\delta < r_k$, the adjusted query point $\hat{\mathbf{Q}}_k$ lies in \mathcal{Q}_k for all $k = 1, \dots, K$. On that account, we redefine the SPSA estimator for (Opt) as

$$\mathbf{V}_k(\mathbf{Q}) = \frac{d_k}{\delta} R(\hat{\mathbf{Q}}) \mathbf{Z}_k, \quad (\text{SPSA})$$

where, in obvious notation, we set $\hat{\mathbf{Q}} = (\hat{\mathbf{Q}}_1, \dots, \hat{\mathbf{Q}}_K)$. The distinguishing feature of (SPSA) is that it is well-posed: *any* query point $\hat{\mathbf{Q}}$ is feasible under (SPSA). Thus, extending the one-dimensional analysis in the beginning of this section, Lemma B.1 claims that the accuracy of the estimator (SPSA) is uniformly bounded as $\|\mathbb{E}[\mathbf{V}_k(\mathbf{Q}) - \nabla R(\mathbf{Q})]\|_* = \mathcal{O}(\delta)$. In the rest of this section, we exploit this property to derive and analyze a first *gradient-free* variant of (MXL).

B. A gradient-free matrix exponential learning scheme

To integrate the gradient estimator (SPSA) as a subroutine of (MXL), we will use a (non-increasing) query radius sequence δ_t satisfying the basic feasibility condition:

$$\delta_t < \min_k r_k = 1/\sqrt{M(M-1)} \quad \text{for all } t \geq 1. \quad (\text{H0})$$

Then, under (MXL), the task of user k at the t -th stage of the algorithm will be given by the following sequence of events:

- 1) Draw a random direction $\mathbf{Z}_{k,t} \in \mathbf{S}^{d_k-1}$.
- 2) Transmit with the covariance matrix $\hat{\mathbf{Q}}_{k,t}$ given by (18).
- 3) Get the achieved throughput $\hat{R}_t = R(\hat{\mathbf{Q}}_t)$.
- 4) Construct the gradient estimate $\mathbf{V}_{k,t}$ given by (SPSA).
- 5) Update $\mathbf{Y}_{k,t}$ and $\mathbf{Q}_{k,t}$ in accordance with (MXL).

The resulting algorithm will be referred to as *gradient-free matrix exponential learning* (MXL0); for a pseudocode implementation, see Alg. 1 above.

Algorithm 1: The MXL0 method

Parameters: γ_t, δ_t
Initialization: $t \leftarrow 1, \mathbf{Y} \leftarrow \mathbf{0};$
 $\forall k: \mathbf{Q}_k \leftarrow (P_k/M_k)\mathbf{I}_k$

1: **Repeat**
2: **For** $k \in \{1, \dots, K\}$ **do** $\text{MXL}\theta_k(\gamma_t, \delta_t)$ **in parallel**
3: $t \leftarrow t + 1$

Routine $\text{MXL}\theta_k(\gamma, \delta)$:
1: **Sample** \mathbf{Z}_k **uniformly over** \mathbb{S}^{d_k-1}
2: **Transmit with** $\hat{\mathbf{Q}}_k \leftarrow \mathbf{Q}_k + \frac{\delta}{r_k}(\mathbf{C}_k - \mathbf{Q}_k) + \delta\mathbf{Z}_k$
3: **Get** $\hat{R} \leftarrow R(\hat{\mathbf{Q}})$
4: **Set** $\mathbf{V}_k \leftarrow \frac{d_k}{\delta}\hat{R}\mathbf{Z}_k$
5: **Set** $\mathbf{Y}_k \leftarrow \mathbf{Y}_k + \gamma\mathbf{V}_k$
6: **Set** $\mathbf{Q}_k \leftarrow \Lambda_k(\mathbf{Y}_k)$

Our first convergence result for MXL0 is as follows:

Theorem 1 (Convergence of MXL0). *Suppose that MXL0 (Alg. 1) is run with non-increasing step-size and query-radius policies satisfying (H0) and*

$$(a) \sum_t \gamma_t = \infty, \quad (b) \sum_t \gamma_t \delta_t < \infty, \quad (c) \sum_t \gamma_t^2 / \delta_t^2 < \infty. \quad (20)$$

Then, with probability 1, the sequence of the users' transmit covariance matrices $\hat{\mathbf{Q}}_t$ converges to the solution set of (Opt).

Theorem 1 provides a strong asymptotic convergence result, but it does not give any indication of the algorithm's convergence speed. To fill this gap, our next result focuses on the algorithm's value convergence rate relative to the maximum achievable transmission rate $R^* = \max R$ of (Opt).

Theorem 2 (Convergence rate of MXL0). *Suppose that MXL0 (Alg. 1) is run for T iterations with constant step-size and query radius parameters of the form $\gamma_t = \gamma/T^{3/4}$ and $\delta_t = \delta/T^{1/4}$, $\delta < 1/\sqrt{M(M-1)}$. Then, the algorithm's ergodic average $\bar{\mathbf{Q}}_T = (1/T)\sum_{t=1}^T \mathbf{Q}_t$ enjoys the bounds:*

(a) *In expectation,*

$$\mathbb{E}[R^* - R(\bar{\mathbf{Q}}_T)] \leq \frac{A(\gamma, \delta)}{T^{1/4}} = \mathcal{O}(T^{-1/4}), \quad (21)$$

where $A(\gamma, \delta) = (K/\gamma) \log M + 4K^2 \lambda \delta + 2^{1-2K} (R^* d)^2 K \gamma / \kappa \delta^2$.

(b) *In probability, for any small enough tolerance $\varepsilon > 0$,*

$$\mathbb{P}\left(R^* - R(\bar{\mathbf{Q}}_T) \geq \frac{A(\gamma, \delta)}{T^{1/4}} + \varepsilon\right) \leq \exp\left(-\frac{2^{2K-5} \delta^2 \varepsilon^2 T^{1/2}}{(R^* K d)^2}\right). \quad (22)$$

In words, Theorem 2 shows that Alg. 1 converges at a rate of $\mathcal{O}(T^{-1/4})$ on average, and the probability of deviating by more than ε from this rate is exponentially small in ε and T . Compared to (MXL), this indicates an increase in the number of iterations required to achieve ε -optimality from $\mathcal{O}(1/\varepsilon^2)$ to $\mathcal{O}(1/\varepsilon^4)$. As we illustrate in detail in Section VI, this performance drop is quite significant and makes MXL0 prohibitively slow in practice. The rest of our paper is devoted precisely to bridging this vital performance gap.

IV. ACCELERATED MXL WITHOUT GRADIENT INFORMATION

Going back to the heuristic discussion of MXL0 in the previous section, we see that the one-shot estimator v is bounded as $|v| \leq \sup |f|/\delta = \mathcal{O}(1/\delta)$. This unveils a significant trade-off between the $\mathcal{O}(\delta)$ bias of the estimator and its $\mathcal{O}(1/\delta)$ deviation from the true derivative: the more accurate v becomes (smaller bias), the less precise it will be (higher variance). In the context of iterative optimization algorithms, this *bias-variance dilemma* induces strict restrictions on the design of the query-radius and step-size policies, with deleterious effects on the algorithm's convergence rate (cf. Sections III and VI). Motivated by this drawback of the SPSA approach, we proceed in the sequel to design a gradient estimator which requires a single function query per iteration, whilst at the same time enjoying a uniform bound on the norms of the estimates.

A. SPSA with callbacks

To proceed with our construction, let z take the value -1 or $+1$ with equal probability, and consider the estimator

$$v_\rho(x) = \frac{f(x + \delta z) - \rho}{\delta} z. \quad (23)$$

The offset value ρ is decided *a priori*, independently of the random variable z , so that $\mathbb{E}[\rho z] = \rho \mathbb{E}[z] = 0$. In turn, this implies that $\mathbb{E}[v_\rho(x)] = \hat{v}(x)$, and hence:

$$\|\mathbb{E}[v_\rho(x) - f'(x)]\| \leq \lambda \delta / 2 \quad (24)$$

i.e., the accuracy (bias) of $v_\rho(x)$ is again $\mathcal{O}(\delta)$.

The novelty of (23) is as follows: if we take $\rho = f(x)$, then $|v_\rho(x)| = (1/\delta)|f(x + \delta z) - f(x)| \leq L$ where L denotes the Lipschitz constant of f , so the choice $\rho = f(x)$ would be ideally suited for our purposes; however, taking $\rho = f(x)$ would also involve an additional function query. To circumvent this, we will instead approximate $f(x)$ with the closest available surrogate, namely the function value observed at the previous iteration of the process.

To make this precise in our MIMO context, we will consider the *enhanced SPSA estimator*

$$\mathbf{V}_{k,t} = \frac{d_k}{\delta_t} [R(\hat{\mathbf{Q}}_t) - R(\hat{\mathbf{Q}}_{t-1})] \mathbf{Z}_{k,t}, \quad (\text{SPSA+})$$

where:

- 1) δ_t is the given query radius at time t .
- 2) $\mathbf{Z}_{k,t}$ is drawn randomly from the sphere \mathbb{S}^{d_k-1}
- 3) $\hat{\mathbf{Q}}_t$ is the transmit covariance matrix defined along (18).

Then, integrating (SPSA+) in the chassis of MXL, we obtain a similarly enhanced version of MXL0, which we call *gradient-free MXL algorithm with callbacks* (MXL0⁺). For concreteness, we present a pseudocode implementation of the resulting method in Alg. 2.

In terms of parameter values, MXL0⁺ supports a broad class of policies satisfying the so-called Robbins–Monro conditions:

$$(a) \sum_t \gamma_t = \infty, \quad (b) \sum_t \gamma_t^2 < \infty. \quad (\text{H1})$$

Algorithm 2: The MXL0⁺ method

Parameters: γ_t, δ_t
Initialization: $t \leftarrow 1, \mathbf{Y} \leftarrow \mathbf{0};$
 $\forall k: \mathbf{Q}_k \leftarrow (P_k/M_k)\mathbf{I}_k, \rho_k \leftarrow R(\mathbf{Q})$

1: Repeat
2: For $k \in \{1, \dots, K\}$ **do** MXL0⁺(γ_t, δ_t) **in parallel**
3: $t \leftarrow t + 1$

Routine MXL0⁺(γ, δ) :

1: Sample \mathbf{Z}_k **uniformly over** \mathcal{S}^{d_k-1}
2: Transmit with $\hat{\mathbf{Q}}_k \leftarrow \mathbf{Q}_k + \frac{\delta}{r_k}(\mathbf{C}_k - \mathbf{Q}_k) + \delta\mathbf{Z}_k$
3: Get $\hat{R} \leftarrow R(\hat{\mathbf{Q}})$
4: Set $\mathbf{V}_k \leftarrow \frac{d_k}{\delta}(\hat{R} - \rho_k)\mathbf{Z}_k$
5: Set $\rho_k \leftarrow \hat{R}$
6: Set $\mathbf{Y}_k \leftarrow \mathbf{Y}_k + \gamma\mathbf{V}_k$
7: Set $\mathbf{Q}_k \leftarrow \Lambda_k(\mathbf{Y}_k)$

In addition, MXL0⁺ also requires the following precautions regarding the allowable step-size and query-radius sequences:

$$\sum_t \gamma_t \delta_t < \infty, \quad (\text{H2})$$

$$\sup_t \gamma_t / \delta_{t+1} < 2/(dLK), \quad (\text{H3})$$

$$\sup_t \delta_t / \delta_{t+1} < \infty, \quad (\text{H4})$$

Of the above conditions, (H3)–(H4) guarantee the uniform boundedness of the gradient estimator, while (H2) is an additional condition needed for convergence of the algorithm.

In practice, these conditions are easy to verify when $\gamma_t = \gamma/t^\alpha$ and $\delta_t = \delta/t^\beta$ for some $\alpha, \beta > 0$. In this case, the conditions (H0)–(H4) reduce to:

$$(dLK/2)\gamma < \delta < 1/\sqrt{M(M-1)}, \quad (\text{Ha})$$

$$0 \leq \beta \leq \alpha \leq 1 \quad \text{and} \quad \alpha + \beta > 1, \quad (\text{Hb})$$

With all this in hand, we are finally in a position to state our main convergence results for the MXL0⁺ algorithm. We begin by establishing the algorithm's almost sure convergence:

Theorem 3 (Convergence of MXL0⁺). *Suppose that MXL0⁺ (Alg. 2) is run with step-size and query-radius policies satisfying (H0)–(H4). Then, with probability 1, the sequence of the users' transmit covariance matrices $\hat{\mathbf{Q}}_t$ converges to the solution set of (Opt).*

As in the case of Theorem 1, Theorem 3 provides a strong asymptotic convergence result, but it leaves open the crucial question of the algorithm's convergence speed. Our next result justifies the introduction of (SPSA+) and shows that Alg. 2 achieves the best of both worlds: one-shot throughput measurements with an $\tilde{\mathcal{O}}(1/\sqrt{T})$ convergence rate.

Theorem 4 (Convergence rate of MXL0⁺). *Suppose that MXL0⁺ (Alg. 2) is run for T iterations. We then have:*

1) If $\gamma_t = \gamma/\sqrt{t}$ and $\delta_t = \delta/\sqrt{t}$ with γ and δ satisfying (Ha):

$$\mathbb{E}[R^* - R(\bar{\mathbf{Q}}_T)] = \mathcal{O}\left(\frac{\log T}{\sqrt{T}}\right). \quad (26)$$

2) If $\gamma_t = \gamma/\sqrt{T}$ and $\delta_t = \delta/\sqrt{T}$ with γ and δ satisfying (Ha):

TABLE I: Parameters of MXL0⁺ for Corollary 1

a) $\gamma = \frac{\sqrt{\log M/(dLK^2)}}{\sqrt{\lambda} + \sqrt{2dLK}}; \quad \delta = \frac{\sqrt{(dL/\lambda)\log M}}{2}; \quad T \geq \frac{LM^4 \log M}{4\lambda}$
b) $\gamma = \frac{\phi(\alpha)}{\sqrt{L}} \left[\sqrt{2Ld\phi(\alpha)} + \sqrt{2/\log(1/\alpha)\lambda} \right]^{-1} \frac{\sqrt{\log M}}{K\sqrt{d}};$ $\delta = \frac{\phi(\alpha)}{2} \sqrt{L/\lambda \sqrt{\log(1/\alpha)/2} d \log M};$ $T = 4\phi^4(\alpha)L^2 \left[1 + \frac{1}{\phi(\alpha)d} \sqrt{2\lambda/L \sqrt{2/\log(1/\alpha)}} \right]^2 \left(\frac{\log(1/\alpha)K^4 d^3 \log M}{\varepsilon^2} \right);$ with $\phi(\alpha) = \left[1/\sqrt{\log(1/\alpha)} + 4/\sqrt{\log(M)} \right]^{1/2}$

a) In expectation,

$$\mathbb{E}[R^* - R(\bar{\mathbf{Q}}_T)] \leq \frac{B(\gamma, \delta)}{\sqrt{T}} = \mathcal{O}\left(\frac{1}{\sqrt{T}}\right), \quad (27)$$

where $B(\gamma, \delta) = (K/\gamma) \log M + 4K^2 \lambda \delta + \frac{8Kd\gamma}{[2/(dLK) - \gamma/\delta]^2}$.

b) In probability, for any small enough tolerance $\varepsilon > 0$,

$$\mathbb{P}\left(R^* - R(\bar{\mathbf{Q}}_T) \geq \frac{B(\gamma, \delta)}{\sqrt{T}} + \varepsilon\right) \leq \exp\left(-\frac{\varepsilon^2 T}{C(\gamma, \delta)}\right), \quad (28)$$

where $C(\gamma, \delta) = 2^9 dK^2/[2/(dLK) - \gamma/\delta]^2$.

Importantly, Theorem 4 shows that MXL0⁺ recovers the $\mathcal{O}(1/\sqrt{T})$ convergence rate of MXL with *full* gradient information, even though the network's users are no longer assumed to have *any* access to a gradient oracle. In fact, the guarantees of Theorem 4 can be optimized further by finetuning the choice of γ and δ ; doing just that (and referring to Appendix D for the details), we have:

Corollary 1. *Suppose that MXL0⁺ is run with $\gamma_t = \gamma/\sqrt{t}$, $\delta_t = \delta/\sqrt{t}$, and T, γ, δ as in Table I. Then:*

a) In expectation, we have:

$$\mathbb{E}[R^* - R(\bar{\mathbf{Q}}_T)] \leq 2L \left(1 + \frac{2^{3/4} \sqrt{\lambda/L}}{d} \right) \sqrt{\frac{K^4 M^6 \log M}{T}}. \quad (29)$$

b) In probability, given a small enough tolerance $\varepsilon > 0$ and a confidence level $1 - \alpha \in (0, 1)$, we have:

$$\mathbb{P}(R^* - R(\bar{\mathbf{Q}}_T) \leq \varepsilon) \geq 1 - \alpha. \quad (30)$$

An important feature of the convergence rate guarantee (30) is that it does not depend on the number of antennas N at the receiver. As such, Alg. 2 exhibits a *scale-free* behavior relative to N , which makes it particularly appealing for distributed massive-MIMO systems. In the next section, we further relax the requirement that all users update their transmit covariance matrices in a synchronous manner, and we derive a fully distributed version of the MXL0⁺ algorithm.

V. DISTRIBUTED IMPLEMENTATION

In this section, we propose a distributed variant of the MXL0⁺ method which can account for randomized and asynchronous user decisions (independent or in alternance with other users). Specifically, we now assume that, at each stage of the process, only a random subset of users perform an update of their individual covariances matrices, while the remaining users maintain the same covariance matrix, without updating.

Algorithm 3: The asynchronous MXL0⁺ (AMXL0⁺) method

Parameters: Π, γ_t, δ_t
Initialization: $t \leftarrow 1, \mathbf{Y} \leftarrow \mathbf{0};$
 $\forall k: \mathbf{Q}_k \leftarrow (P_k/M_k) \mathbf{I}_k, \rho_k \leftarrow R(\mathbf{Q})$

1: Repeat
2: | Draw set of active users U according to Π
3: | For $k \in \{1, \dots, K\}$ do in parallel
4: | | If $k \in U$ then $\text{MXL}\hat{\theta}_k^*(\gamma_t, \delta_t)$ else Pass_k
5: | $t \leftarrow t + 1$

Routine Pass_k :
1: | Transmit with \mathbf{Q}_k
2: | Get $\rho_k \leftarrow R(\mathbf{Q})$

To state this formally, suppose that a random subset of users $U_t \subseteq \mathcal{K} \equiv \{1, \dots, K\}$ is drawn at stage t following an underlying probability law $\Pi \equiv (\Pi_U)_{U \subseteq \mathcal{K}}$ (i.e., $U \subseteq \mathcal{K}$ is drawn with probability Π_U). From the distributed perspective of individual users, we write $\pi_k = \sum_{U \ni k} \Pi_U$ to denote the *marginal probability* that user k updates their covariance at any stage t ; as such, the participation of all users is enforced by imposing the condition $\pi_k > 0$. We thus obtain the asynchronous MXL0⁺ scheme:

$$\begin{aligned} \mathbf{Q}_t &= \mathbf{\Lambda}(\mathbf{Y}_t), \\ \mathbf{Y}_{t+1} &= \mathbf{Y}_t + \gamma_t \hat{\mathbf{V}}_t, \end{aligned} \quad (\text{AMXL0}^+)$$

where $\hat{\mathbf{V}}_{k,t} = \mathbf{V}_{k,t}$ if $k \in U_t$, and $\hat{\mathbf{V}}_{k,t} = \mathbf{0}$ otherwise. For a pseudocode implementation, see also Alg. 3 above.

As we show below, AMXL0⁺ recovers the $\mathcal{O}(1/\sqrt{T})$ convergence rate of MXL0⁺, despite being distributed across users:

Theorem 5 (Convergence rate of AMXL0⁺). *Suppose that AMXL0⁺ (Alg. 3) is run for T iterations. We then have:*

1) If $\gamma_t = \gamma/\sqrt{t}$ and $\delta_t = \delta/\sqrt{t}$ with γ and δ satisfying (Ha):

$$\mathbb{E}[R^* - R(\bar{\mathbf{Q}}_T)] = \mathcal{O}\left(\frac{\log T}{\sqrt{T}}\right). \quad (31)$$

2) If $\gamma_t = \gamma/\sqrt{T}$ and $\delta_t = \delta/\sqrt{T}$ with γ and δ satisfying (Ha):

a) In expectation,

$$\mathbb{E}[R^* - R(\bar{\mathbf{Q}}_T)] \leq \frac{B_\pi(\gamma, \delta)}{\sqrt{T}} = \mathcal{O}\left(\frac{1}{\sqrt{T}}\right), \quad (32)$$

where $B_\pi(\gamma, \delta) = \sum_{k=1}^K \frac{\log M_k}{\pi_k \gamma} + 4K^2 \lambda \delta + \frac{8Kd\gamma}{[2/(dLK) - \gamma/\delta]^2}$.

b) In probability, for any small enough tolerance $\varepsilon > 0$,

$$\mathbb{P}\left(R^* - R(\bar{\mathbf{Q}}_T) \geq \frac{B_\pi(\gamma, \delta)}{\sqrt{T}} + \varepsilon\right) \leq \exp\left(-\frac{\varepsilon^2 T}{C_\pi(\gamma, \delta)}\right), \quad (33)$$

where $C_\pi(\gamma, \delta) = \left[1 + \frac{\nu_\pi}{2} + \frac{\nu_\pi d^{3/2} L K \gamma \delta}{2\delta - dLK\gamma}\right]^2 C(\gamma, \delta)$, with $\nu_\pi = K^{-1} \sum_{k=1}^K \max(1, \pi_k^{-1} - 1)$ and $C(\gamma, \delta)$ as in Theorem 4.

Note here that the quantity $B_\pi(\gamma, \delta)$ above only differs from its counterpart $B(\gamma, \delta)$ of Theorem 4 in the first term, which measures the cost of asynchronicity in terms of expected convergence. A similar increase in the deviation from the mean transpires through an impeding factor in the expression for $C_\pi(\gamma, \delta)$, quantifying the impact of asynchronicity in both mean and fluctuation terms.

TABLE II: Parameters of UCD-MXL0⁺ of Corollary 2

a) $\gamma = \left[1 + \sqrt{\frac{2LK}{\lambda} d}\right]^{-1} \sqrt{\frac{\log M}{\lambda L K d}}; \delta = \frac{1}{2} \sqrt{\frac{LKd \log M}{\lambda}}; T \geq \frac{1}{4\lambda} [LKM^4 \log M]$

b) $\gamma = \hat{\psi}(\alpha) \left[\sqrt{\hat{\chi}(\alpha) L \lambda} + 2 \log^{3/8}(\frac{1}{\alpha}) \hat{\chi}(\alpha) \hat{\psi}(\alpha) L [Kd]^{3/4}\right]^{-1} \left(\frac{\log^{1/8}(1/\alpha) \sqrt{\log M}}{[Kd]^{3/4}}\right);$
 $\delta = \left(\frac{\hat{\psi}(\alpha)}{2} \sqrt{\frac{L}{\hat{\chi}(\alpha) \lambda}}\right) \left[\sqrt{\log(1/\alpha)} K d\right]^{1/4} \sqrt{\log M};$
 $T = 16L^2 \left[\hat{\psi}^2(\alpha) + \frac{\hat{\psi}(\alpha) \sqrt{\lambda [\hat{\chi}(\alpha) L]}}{\log^{3/8}(1/\alpha) K^{3/4} d}\right]^2 \left(\frac{\log(1/\alpha) K^6 d^3 \log M}{\varepsilon^2}\right);$
with $\hat{\psi}(\alpha) = \left[\frac{\hat{\chi}(\alpha)}{\sqrt{K} \sqrt{\log(1/\alpha)}} + \sqrt{2/\log(M)} (1 + 1/K)\right]^{1/2},$
 $\hat{\chi}(\alpha) = \left[\sqrt{2}(1 - 1/K) + \frac{1}{2K \sqrt{\log(1/\alpha)}}\right]^{1/2}$

In Appendix E, we show how the parameters (γ, δ) can be optimized for general Π ; for concreteness, we present below the particular case where at any stage each user is active with probability $\pi_k = 1/K$:

Corollary 2 (Uniform AMXL0⁺, $K \geq 2$). *Suppose that AMXL0⁺ is run with $\pi_1 = \dots = \pi_K = 1/K$, $\gamma_t = \gamma/\sqrt{t}$, $\delta_t = \delta/\sqrt{t}$, and T, γ, δ as in Table II. Then:*

a) In expectation, we have:

$$R^* - \mathbb{E}\left[R(\bar{\mathbf{Q}}_T)\right] \leq 2L \left(1 + \sqrt{\lambda/L}\right) \sqrt{\frac{K^5 M^6 \log M}{T}}. \quad (34)$$

b) In probability, given a small enough tolerance $\varepsilon > 0$ and a confidence level $1 - \alpha \in (0, 1)$, we have:

$$\mathbb{P}(R^* - R(\bar{\mathbf{Q}}_{T'}) \leq \varepsilon) \geq 1 - \alpha. \quad (35)$$

Remark 2 (Coordinate descent). The case $\Pi_{\{1\}} = \dots = \Pi_{\{K\}} = 1/K$ where a single user is active at each time step with probability $\pi_k = 1/K$ covers the alternated optimization scheme known as (uniform) ‘‘coordinate descent’’ (UCD-MXL0⁺)—the coordinates in this context refer to the wireless users. In this regard, Corollary 2 provides us with a quantification of the impact of alternation on the convergence speed of MXL0⁺. Looking for instance at Corollaries 1(a) and 2(a), we observe that the expected convergence of the time average, if regarded as a function of the total number n of user updates, is $\mathcal{O}(\sqrt{K^5 M^6 \log M/n})$ both for the synchronized algorithm MXL0⁺ and for UCD-MXL0⁺. The impact of the network size K on the number of user updates needed for ε -convergence with probability $1 - \alpha$, however, is more pronounced by an order of magnitude for UCD-MXL0⁺, $\Theta(\log(1/\alpha) K^6 M^6 \log M/\varepsilon^2)$, than it is for MXL0⁺, $\Theta(\log(1/\alpha) K^5 M^6 \log M/\varepsilon^2)$.

VI. NUMERICAL EXPERIMENTS

In this section, we perform a series of numerical experiments to validate our results in realistic network conditions.

We begin by examining the convergence of the proposed algorithms over a randomly generated MIMO system consisting of 20 heterogeneous users equipped with 3 antennas on average, and all transmitting to a common receiver with 16 receive antennas. The results of our experiments are reported in Fig. 1 where we plot the users’ achieved throughput under the gradient-based MXL algorithm and the three gradient-free algorithms discussed in the previous sections, MXL0, MXL0⁺ and AMXL0⁺ (Algs. 1–3 respectively, the third in the coordinate descent form UCD-MXL0⁺ discussed in Remark 2).

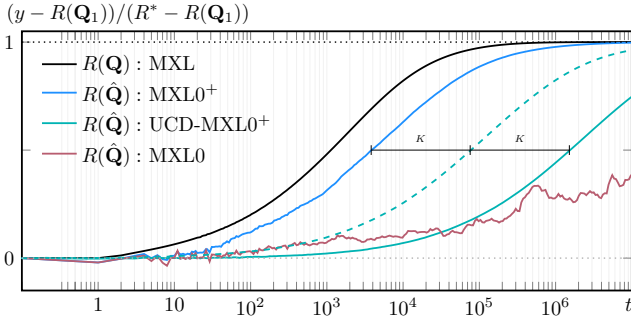


Fig. 1: Achieved rate under gradient-based and gradient-free MXL ($N = 16$, $K = 20$). Despite the complete lack of gradient information, MXL0⁺ remains competitive to the gradient-based MXL algorithm.

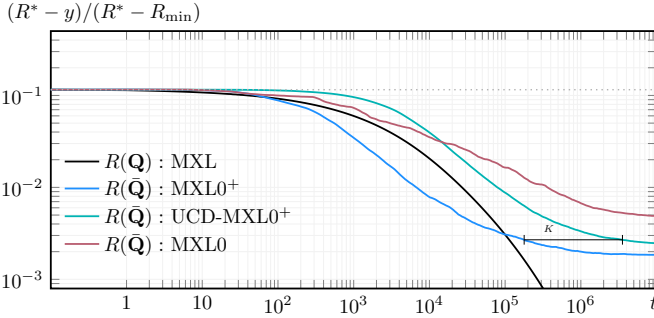


Fig. 2: Convergence speed of the methods under study ($N = 16$, $K = 20$). The callback mechanism in MXL0⁺ greatly improves performance over MXL0, reaching gradient-based performance levels.

The gradient-free algorithms are all run with decreasing step-size and query-radius policies chosen according to Theorems 1 and 3, while MXL is run with a tight step-size policy as in [14].⁶

In Fig. 1, we see that the SPSA-based MXL0 algorithm achieves some moderate gains over time, but it has not converged even after 10^7 iterations. By contrast, the enhanced MXL0⁺ and UCD-MXL0⁺ algorithms converge much faster; MXL0⁺ in particular remains competitive to the *gradient-based* MXL method, despite the complete lack of gradient feedback. We also see that shifting the UCD-MXL0⁺ curve left by $\log 20$ on the semi-log graph (dotted line) discloses the actual performance of UCD-MXL0⁺ in terms of the number of updates per user. The remaining $\log 20$ gap with the MXL0⁺ curve suggests that the loss in efficiency due to full asynchronicity amounts to a factor $K = 20$ on average.

Figure 2 gives us a deeper insight into the performance of the algorithms. The gradient-free algorithms are now run with constant step size and query radius, with focus on $R(\hat{Q}_t)$. The simulations show (UCD-)MXL0⁺ to be competitive with MXL, despite the complete lack of gradient information (and related overheads). A close inspection of the slopes of the various curves on the log-log graph reveals the $\mathcal{O}(1/\sqrt[4]{t})$ complexity of MXL0 and the $\mathcal{O}(1/\sqrt{t})$ complexity of (UCD-)MXL0⁺, in full accordance with Theorems 2, 4 and 5. The $\log 20$ shift between UCD-MXL0⁺ and MXL0⁺ predicted in Remark 2 can also be clearly observed.

⁶In view of (H3), the step-size and query radius policies of (UCD-)MXL0⁺ must be designed in concert. Our gradient-free experiments proved most effective when conducted under the rule of thumb $\gamma_t = 0.1 \delta_t$ at all t .

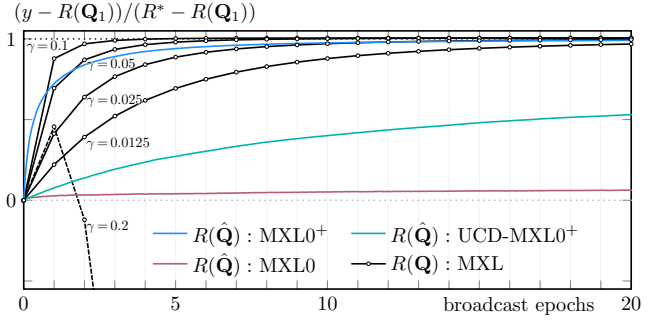


Fig. 3: Overhead of the algorithms under study in a large network ($K = 50$, $N = 128$). When normalized for overhead, MXL0⁺ matches the performance of finely tuned gradient-based methods.

Finally, Fig. 3 provides a normalized analysis in terms of the overhead needed by the algorithms for convergence over a sizeable network with $N = 128$ receive antennas and $K = 50$ transmitters. Here, broadcasting a full (dense) gradient matrix would require $N^2 = 32$ MB of 16-bit data per broadcast, so we examine the algorithms' convergence speed in terms of the full 'broadcast epochs' required for convergence. For benchmarking purposes, we ran MXL with a constant step-size $\gamma_t \equiv \gamma$ (the most principled choice given the smoothness of R), whereas the gradient-free algorithms were coupled with a mixed policy (constant at first, then decreasing) to conjugate immediate gains in throughput with convergence in the long term. Quite remarkably, we see that MXL0⁺ remains competitive with—outperforms even—the fastest implementations of MXL. As expected, UCD-MXL0⁺ was essentially $K = 50$ times greedier than MXL0⁺ in terms of function queries. We however were unable to observe any significant headway from MXL0 in the considered time window.

VII. DISCUSSION

In this paper, we proposed a series of zeroth-order matrix exponential learning schemes for multi-user MIMO systems that circumvent the need for gradient-based feedback (perfect, noisy, or otherwise). Gradient estimation methods based on conventional simultaneous perturbation stochastic approximation (SPSA) techniques lead to an $\mathcal{O}(1/T^{1/4})$ convergence rate, which is catastrophically slow for large MIMO systems. To overcome this deficiency, we introduced an effective variance reduction mechanism which achieves an $\mathcal{O}(1/T^{1/2})$ convergence rate through the reuse of previous throughput measurements. In this regard, the proposed algorithm, *gradient-free MXL algorithm with callbacks* (MXL0⁺), enjoys the best of several worlds: it achieves optimal transmission rates with minimal feedback (and, in particular, no gradient information), it matches the convergence speed of much more expensive gradient-based methods, all the while remaining simple in principle and easy to implement.

Although we focused on the throughput maximization problem in the MIMO multiple-access channel, the gradient-free methodology presented in this work can be easily tailored to a wide range of resource allocation problems that arise in signal processing and wireless communications (from power control to energy efficiency). We defer these applications to the future.

APPENDIX
TECHNICAL PROOFS

A. Matrix exponential learning as a dual averaging scheme

In our developments, the space of the covariance matrices of each user is equipped with the nuclear norm, given for any Hermitian matrix \mathbf{Q} by $\|\mathbf{Q}\| = \text{tr}(\sqrt{\mathbf{Q}\mathbf{Q}})$, and equivalent to the L_1 -norm of the vector of the eigenvalues of \mathbf{Q} . The dual of the nuclear norm, $\|\mathbf{Q}\|_* = \max_{\mathbf{Q}'} \{\text{tr}(\mathbf{Q}\mathbf{Q}') : \|\mathbf{Q}'\| \leq 1\}$, reduces to the L_∞ -norm of the vector of eigenvalues. For every $m \times m$ Hermitian matrix \mathbf{Q} , one has

$$\|\mathbf{Q}\|_* \leq \|\mathbf{Q}\|_2 \leq \|\mathbf{Q}\| \leq \sqrt{m}\|\mathbf{Q}\|_2 \leq m\|\mathbf{Q}\|_*, \quad (\text{A.1})$$

where $\|\mathbf{Q}\|_2 = \sqrt{\text{tr}(\mathbf{Q}\mathbf{Q})}$ denotes the (Frobenius) L^2 -norm of \mathbf{Q} . From the global perspective of matrix arrangements $\mathbf{Q} = (\mathbf{Q}_1, \dots, \mathbf{Q}_K)$ —now regarded as block diagonal covariance matrices—the trace norm and its dual naturally extend as

$$\|\mathbf{Q}\| = \sum_{k=1}^K \|\mathbf{Q}_k\|, \quad \|\mathbf{Q}\|_* = \max_{k \in \{1, \dots, K\}} \|\mathbf{Q}_k\|_*. \quad (\text{A.2})$$

We now derive the matrix exponential learning step and some properties of it. To this end, we place ourselves in the compact set $\mathcal{Q} = \{\mathbf{Q} \in \text{Herm}(M) : \text{tr}(\mathbf{Q}) = 1, \mathbf{Q} \geq 0\}$ of the M -dimensional positive semidefinite Hermitian matrices with unit trace—the parameter M stands for the number of antennas of any of the K users. Let the inner product $\langle \mathbf{Y}, \mathbf{Q} \rangle = \text{tr}(\mathbf{Y}\mathbf{Q})$ denote the value at $\mathbf{Q} \in \mathcal{Q}$ of the linear function induced by $\mathbf{Y} \in \mathcal{Y}$, where $\mathcal{Y} = \{\mathbf{Z} \in \text{Herm}(M) : \text{tr}(\mathbf{Z}) = 0\}$ is tangent to \mathcal{Q} . For any differentiable function f on $\text{Herm}(M)$, we denote by $\nabla f : \mathcal{Q} \mapsto \mathcal{Y}$ the *orthogonal projection* of the gradient ∇f on the tangent space \mathcal{Y} , given by $\nabla f = \nabla f - \text{tr}(\nabla f)\mathbf{I}$.

Lemma A.1.

(i) The regularization function⁷ $h(\mathbf{Q}) = \text{tr}(\mathbf{Q} \log \mathbf{Q})$ is 1-strongly convex over \mathcal{Q} with respect to $\|\cdot\|$.

(ii) The conjugate of h , $h^* : \mathcal{Y} \mapsto \mathbb{R}$, defined by

$$h^*(\mathbf{Y}) = \max_{\mathbf{Q} \in \mathcal{Q}} \{\langle \mathbf{Y}, \mathbf{Q} \rangle - h(\mathbf{Q})\}, \quad (\text{A.3})$$

is differentiable with gradient $\nabla h^* = \Lambda$, where Λ is the exponential learning mapping defined by

$$\Lambda(\mathbf{Y}) = \frac{\exp(\mathbf{Y})}{\text{tr}(\exp(\mathbf{Y}))}. \quad (\text{A.4})$$

(iii) For $\mathbf{Q} \in \mathcal{Q}$ and $\mathbf{Y} \in \mathcal{Y}$,

$$\mathbf{Q} = \Lambda(\mathbf{Y}) \Leftrightarrow \mathbf{Y} = \nabla h(\mathbf{Q}). \quad (\text{A.5})$$

(iv) h^* is 1-smooth with respect to the dual norm $\|\cdot\|_*$.

Proof. We refer to [27] for the strong convexity of h . For (ii), the differentiability of h^* is a consequence of Danskin's theorem (e.g. [28]), which, besides, gives us the gradient of (A.3),

$$\nabla h^*(\mathbf{Y}) = \arg \max_{\mathbf{Q} \in \mathcal{Q}} \{\langle \mathbf{Y}, \mathbf{Q} \rangle - h(\mathbf{Q})\}. \quad (\text{A.6})$$

Relaxing the constraint $\text{tr}(\mathbf{Q}) - 1 = 0$ in the subproblem (A.6) and using $\nabla h(\mathbf{Q}) = \mathbf{I} + \log \mathbf{Q}$ yields the stationarity condition

$$\log \mathbf{Q} - \mathbf{Y} + (1 + \nu)\mathbf{I} = 0, \quad (\text{S})$$

⁷The regularizer h , known as the negative Von Neumann quantum entropy, is considered with convention $0 \log 0 = 0$.

where $\nu \in \mathbb{R}$ is the Lagrange multiplier related to the constraint. Condition (S) rewrites as $\mathbf{Q} = \exp(-(1 + \nu)) \exp(\mathbf{Y})$, which implies the primal feasibility condition $\mathbf{Q} \geq 0$. The remaining KKT conditions $\text{tr}(\mathbf{Q}) - 1 \leq 0$ and $\nu(\text{tr}(\mathbf{Q}) - 1) = 0$ yield $\nu = \log(\text{tr}(\exp(\mathbf{Y}))) - 1$, and $\mathbf{Q} = \Lambda(\mathbf{Y})$ as the unique maximizer of (A.6), which completes the proof of (ii).

Now, it follows from (A.6) that, for any $\mathbf{Y} \in \mathcal{Y}_k$, one has $\mathbf{Q} = \Lambda(\mathbf{Y})$ if and only if $\langle \mathbf{Y}, \mathbf{Q}' \rangle - h(\mathbf{Q}') \leq \langle \mathbf{Y}, \mathbf{Q} \rangle - h(\mathbf{Q})$ holds for all $\mathbf{Q}' \in \mathcal{Q}$, i.e., iff \mathbf{Y} is a subgradient of h at \mathbf{Q} . Claim (iii) follows by differentiability of h .

Finally, (iv) is a property of convex conjugation [29–31]. Indeed, let $\mathbf{Y}, \mathbf{Y}' \in \mathcal{Y}$ and $\mathbf{Q} = \Lambda(\mathbf{Y})$. By convexity,

$$h(\mathbf{Q}') \geq h(\mathbf{Q}) + \langle \nabla h(\mathbf{Q}), \mathbf{Q}' - \mathbf{Q} \rangle + \frac{1}{2}\|\mathbf{Q}' - \mathbf{Q}\|^2 \quad (\text{A.7})$$

holds for any $\mathbf{Q}' \in \mathcal{Q}$. It follows that

$$\begin{aligned} h^*(\mathbf{Y}') &\stackrel{(\text{A.3})}{=} \max_{\mathbf{Q}' \in \mathcal{Q}} \{\langle \mathbf{Y}', \mathbf{Q}' \rangle - h(\mathbf{Q}')\} \\ &\stackrel{(\text{A.7})}{\leq} \max_{\mathbf{Q}' \in \mathcal{Q}} \{\langle \mathbf{Y}', \mathbf{Q}' \rangle - h(\mathbf{Q}) - \langle \nabla h(\mathbf{Q}), \mathbf{Q}' - \mathbf{Q} \rangle - \frac{1}{2}\|\mathbf{Q}' - \mathbf{Q}\|^2\} \\ &\stackrel{(\text{A.5})}{=} \langle \mathbf{Y}, \mathbf{Q} \rangle - h(\mathbf{Q}) + \langle \mathbf{Y}' - \mathbf{Y}, \mathbf{Q} \rangle + \max_{\mathbf{Q}' \in \mathcal{Q}} \{\langle \mathbf{Y}' - \mathbf{Y}, \mathbf{Q}' - \mathbf{Q} \rangle - \frac{1}{2}\|\mathbf{Q}' - \mathbf{Q}\|^2\} \\ &\stackrel{(\text{A.6})}{\leq} h^*(\mathbf{Y}) + \langle \mathbf{Y}' - \mathbf{Y}, \nabla h^*(\mathbf{Y}) \rangle + \frac{1}{2}\|\mathbf{Y}' - \mathbf{Y}\|^2 \end{aligned} \quad (\text{A.8})$$

and h^* is 1-smooth. Equivalently, (A.8) rewrites as [32]

$$\|\Lambda(\mathbf{Y}) - \Lambda(\mathbf{Y}')\| \leq \|\mathbf{Y} - \mathbf{Y}'\|_* \quad \forall \mathbf{Y}, \mathbf{Y}' \in \mathcal{Y}_k. \quad (\text{A.9})$$

■

We now consider the Fenchel primal-dual coupling $F : \mathcal{Q} \times \mathcal{Y} \mapsto \mathbb{R}$ associated with the entropic regularizer h .

Lemma A.2. The Fenchel coupling

$$F(\mathbf{Q}, \mathbf{Y}) = h(\mathbf{Q}) + h^*(\mathbf{Y}) - \langle \mathbf{Y}, \mathbf{Q} \rangle \quad (\text{A.10})$$

satisfies the following properties. For $\mathbf{Q} \in \mathcal{Q}$ and $\mathbf{Y}, \mathbf{Y}' \in \mathcal{Y}$,

$$F(\mathbf{Q}, \mathbf{Y}') \leq F(\mathbf{Q}, \mathbf{Y}) + \langle \mathbf{Y}' - \mathbf{Y}, \Lambda(\mathbf{Y}) - \mathbf{Q} \rangle + \frac{1}{2}\|\mathbf{Y}' - \mathbf{Y}\|_*^2, \quad (\text{A.11a})$$

$$F(\mathbf{Q}, \mathbf{Y}) \geq \frac{1}{2}\|\mathbf{Q} - \Lambda(\mathbf{Y})\|^2, \quad (\text{A.11b})$$

$$F(\mathbf{Q}, \mathbf{Y}) \geq 0 \text{ with } F(\mathbf{Q}, \mathbf{Y}) = 0 \Leftrightarrow \mathbf{Y} = \nabla h(\mathbf{Q}). \quad (\text{A.11c})$$

Proof. Equations (A.11a) and (A.11b) follow from the smoothness of h^* and from the strong convexity of h , respectively. Indeed, we get (A.11a) by combining (A.10) with (A.8), while

$$\begin{aligned} F(\mathbf{Q}, \mathbf{Y}) &\stackrel{(\text{A.10})}{=} \max_{\mathbf{Q}' \in \mathcal{Q}} \{h(\mathbf{Q}) - h(\mathbf{Q}') - \langle \mathbf{Y}, \mathbf{Q} - \mathbf{Q}' \rangle\} \\ &\stackrel{(\text{A.5})}{\geq} h(\mathbf{Q}) - h(\Lambda(\mathbf{Y})) - \langle \nabla h(\Lambda(\mathbf{Y})), \mathbf{Q} - \Lambda(\mathbf{Y}) \rangle \\ &\stackrel{(\text{A.7})}{\geq} \frac{1}{2}\|\mathbf{Q} - \Lambda(\mathbf{Y})\|^2 \end{aligned} \quad (\text{A.12})$$

yields (A.11b). Then, (A.11c) follows from (A.11b) and (A.5). ■

B. The SPSA estimator

This section is concerned with the bias of the gradient estimator defined, for $k = 1, \dots, K$, by

$$\mathbf{V}_k(\mathbf{Q}, \mathbf{Z}; \rho) = \frac{\delta_k}{\delta} [R(\hat{\mathbf{Q}}) - \rho] \mathbf{Z}_k, \quad (\text{B.1})$$

where $\delta > 0$ is a given query radius, $\hat{\mathbf{Q}} = (\hat{\mathbf{Q}}_1, \dots, \hat{\mathbf{Q}}_K)$ is given by (18), $\mathbf{Z} = (\mathbf{Z}_1, \dots, \mathbf{Z}_K)$ with \mathbf{Z}_k sampled uniformly on the

sphere \mathbf{S}^{d_k-1} , and ρ an arbitrary scalar offset quantity independent of \mathbf{Z} . Observe that (B.1) covers the gradient estimators of both MXL0 and MXL0⁺.

The computation of a bound for the bias of estimator (B.1) is based on Stokes' theorem, applied to the sphere \mathbf{S}^{d_k-1} :

$$\int_{\mathbf{S}^{d_k-1}} f(\mathbf{Z}_k) \mathbf{Z}_k d\mu(\mathbf{Z}_k) = \int_{\mathbf{B}^{d_k}} \nabla f(\zeta) d\mu(\zeta), \quad (\text{B.2})$$

where f is any function on $\text{Herm}(M_k)$ and μ denotes the Lebesgue measure. Before proceeding, observe that each test covariance matrix $\hat{\mathbf{Q}}_k$ is bound to the initial matrix \mathbf{Q}_k by $\|\hat{\mathbf{Q}}_k - \mathbf{Q}_k\|_2 \leq 2\delta\|\mathbf{Z}_k\|_2$, where, under our assumption $d_k > 0$, $\|\mathbf{Z}_k\|_* \leq 1/2$ for every $\mathbf{Z}_k \in \mathbf{S}^{d_k-1}$. It follows from (A.1) that any test configuration $\hat{\mathbf{Q}}$ in (SPSA) and (SPSA+) satisfies

$$\|\hat{\mathbf{Q}} - \mathbf{Q}\|_2 \leq 2\delta K, \quad \text{and} \quad \|\hat{\mathbf{Q}} - \mathbf{Q}\| \leq 2\delta K \sqrt{d}. \quad (\text{B.3})$$

Lemma B.1. *The estimator (B.1) satisfies*

$$\|\mathbb{E}[\mathbf{V}_k(\mathbf{Q}, \mathbf{Z}; \rho) - \nabla_k R(\mathbf{Q})]\|_* \leq 2K\lambda_k \delta, \quad (\text{B.4})$$

$$\|\mathbf{V}_k(\mathbf{Q}, \mathbf{Z}; \rho)\|_* \leq \frac{d_k}{2K\delta} \max_{\mathbf{Q}' \in \mathcal{Q}} |R(\mathbf{Q}') - \rho|. \quad (\text{B.5})$$

Proof of Lemma B.1. We argue as in [17, 33]. By introducing the notation $\tilde{\mathbf{Q}}^\delta(\zeta) = (\hat{\mathbf{Q}}_1, \dots, \hat{\mathbf{Q}}_{k-1}, \hat{\mathbf{Q}}_k^\delta(\zeta), \hat{\mathbf{Q}}_{k+1}, \dots, \hat{\mathbf{Q}}_K)$, in which $\hat{\mathbf{Q}}_k^\delta(\zeta) = \mathbf{Q}_k + (\delta/r_k)(\mathbf{C}_k - \mathbf{Q}_k) + \delta\zeta$, we find

$$\begin{aligned} & \|\mathbb{E}[\mathbf{V}_k(\mathbf{Q}, \mathbf{Z}; \rho) - \nabla_k R(\mathbf{Q})]\|_* \\ & \stackrel{(\text{B.1})}{=} \left\| \mathbb{E} \left[\frac{d_k}{\delta} [R(\hat{\mathbf{Q}}) - \rho] \mathbf{Z}_k - \nabla_k R(\mathbf{Q}) \right] \right\|_* \\ & = \left\| \frac{d_k}{\delta} \mathbb{E} [R(\hat{\mathbf{Q}}) \mathbf{Z}_k] - \nabla_k R(\mathbf{Q}) \right\|_* \\ & = \frac{d_k}{\delta} \mathbb{E} \left[\frac{\int_{\mathbf{S}^{d_k-1}} R(\hat{\mathbf{Q}}^\delta(\mathbf{Z}_k)) \mathbf{Z}_k d\mu(\mathbf{Z}_k)}{\text{vol}(\mathbf{S}^{d_k-1})} - \nabla_k R(\mathbf{Q}) \right]_* \\ & \stackrel{(\text{B.6})}{=} \left\| \mathbb{E} \left[\frac{\int_{\mathbf{S}^{d_k-1}} R(\hat{\mathbf{Q}}^\delta(\mathbf{Z}_k)) \mathbf{Z}_k d\mu(\mathbf{Z}_k)}{\delta \text{vol}(\mathbf{B}^{d_k})} - \nabla_k R(\mathbf{Q}) \right] \right\|_* \end{aligned} \quad (\text{B.6})$$

It follows from Stokes' theorem that (B.6) reduces to

$$\begin{aligned} & \|\mathbb{E}[\mathbf{V}_k(\mathbf{Q}, \mathbf{Z}; \rho) - \nabla_k R(\mathbf{Q})]\|_* \\ & \stackrel{(\text{B.2})}{=} \left\| \mathbb{E} \left[\frac{\int_{\mathbf{B}^{d_k}} \delta \nabla_k R(\hat{\mathbf{Q}}^\delta(\zeta)) d\mu(\zeta)}{\delta \text{vol}(\mathbf{B}^{d_k})} - \nabla_k R(\mathbf{Q}) \right] \right\|_* \\ & \leq \mathbb{E} \left[\frac{1}{\text{vol}(\mathbf{B}^{d_k})} \int_{\mathbf{B}^{d_k}} \|\nabla_k R(\hat{\mathbf{Q}}^\delta(\zeta)) - \nabla_k R(\mathbf{Q})\|_* d\mu(\zeta) \right] \\ & \stackrel{(\text{B.1})}{\leq} \frac{\int_{\mathbf{B}^{d_k}} \lambda_{kk} \|\hat{\mathbf{Q}}_k^\delta(\zeta) - \mathbf{Q}_k\|_2 d\mu(\zeta)}{\text{vol}(\mathbf{B}^{d_k})} + \sum_{\ell \neq k} \lambda_{k\ell} \mathbb{E} [\|\hat{\mathbf{Q}}_\ell - \mathbf{Q}_\ell\|_2] \\ & \stackrel{(\text{B.3})}{\leq} \lambda_{kk} \left(1 + \frac{\int_{\mathbf{B}^{d_k}} \|\zeta\|_2 d\mu(\zeta)}{\text{vol}(\mathbf{B}^{d_k})} \right) \delta + 2 \sum_{\ell \neq k} \lambda_{k\ell} \mathbb{E} [\|\mathbf{Z}_\ell\|_2] \delta \\ & \leq \lambda_{kk} \left(\frac{2M_k+1}{M_k+1} \right) \delta + 2 \sum_{\ell \neq k} \lambda_{k\ell} \delta \leq 2K\lambda_k \delta, \end{aligned} \quad (\text{B.7})$$

and we recover (B.4). Then (B.5) is immediate from the definition of $\mathbf{V}_k(\mathbf{Q}, \mathbf{Z}; \rho)$ and the fact that $\|\mathbf{Z}_\ell\|_* \leq 1/2$ for all ℓ . ■

C. Analysis of the MXL0 algorithm

Let \mathcal{Q}^* denote the solution set of (Opt). Given any $\mathbf{Q}^* \in \mathcal{Q}^*$, we consider, for analysis purposes, the Lyapunov function

$$\mathcal{L}(\mathbf{Y}; \mathbf{Q}^*) = \sum_{k=1}^K F(\mathbf{Q}_k^*, \mathbf{Y}_k), \quad (\text{C.1})$$

where F is the Fenchel coupling defined in (A.10). If $\mathcal{F}_{t-1} = (\mathbf{Y}_1, \mathbf{Z}_1, \dots, \mathbf{Y}_{t-1}, \mathbf{Z}_{t-1})$ denotes the history of MXL0 up to step $t-1$, the gradient estimator (B.1) decomposes into

$$\mathbf{V}_{k,t} = \nabla_k R(\mathbf{Q}_t) + \mathbf{B}_{k,t} + \mathbf{U}_{k,t}, \quad (\text{C.2})$$

where $\mathbf{B}_{k,t} = \mathbb{E}[\mathbf{V}_{k,t} | \mathcal{F}_{t-1}] - \nabla_k R(\mathbf{Q}_t)$ is the systematic error on $\mathbf{V}_{k,t}$, bounded by

$$\|\mathbf{B}_{k,t}\|_* \stackrel{(\text{B.4})}{\leq} 2K\lambda_k \delta_t, \quad (\text{C.3})$$

and $\mathbf{U}_{k,t}$ is the random deviation of $\mathbf{V}_{k,t}$ from its expected value $\mathbb{E}[\mathbf{V}_{k,t} | \mathcal{F}_{t-1}]$, so that $\mathbb{E}[\mathbf{U}_{k,t} | \mathcal{F}_{t-1}] = 0$, and

$$\|\mathbf{U}_{k,t}\|_* \leq \|\mathbf{V}_{k,t}\|_* + \mathbb{E}[\|\mathbf{V}_{k,t}\|_* | \mathcal{F}_{t-1}]. \quad (\text{C.4})$$

In our analysis we consider the following random sequence:

$$Z_t = \gamma_t \sum_{k=1}^K \langle \mathbf{U}_{k,t}, \mathbf{Q}_{k,t} - \mathbf{Q}_k^* \rangle. \quad (\text{C.5})$$

Since $|\langle \mathbf{U}_{k,t}, \mathbf{Q}_{k,t} - \mathbf{Q}_k^* \rangle| \leq \|\mathbf{U}_{k,t}\|_* \|\mathbf{Q}_{k,t} - \mathbf{Q}_k^*\| \leq 2\|\mathbf{U}_{k,t}\|_*$, one has

$$\text{a) } \mathbb{E}[Z_t | \mathcal{F}_{t-1}] = 0, \quad \text{b) } |Z_t| \leq 2\gamma_t \sum_{k=1}^K \|\mathbf{U}_{k,t}\|_*. \quad (\text{C.6})$$

Lemma C.1. *Run MXL0/MXL0⁺ for t iterations under (H0).*

(i) *With any step-size and query radius policy (γ_t, δ_t) ,*

$$\begin{aligned} \mathcal{L}(\mathbf{Y}_{t+1}; \mathbf{Q}^*) & \leq \mathcal{L}(\mathbf{Y}_t; \mathbf{Q}^*) - \gamma_t [R^* - R(\mathbf{Q}_t)] + Z_t \\ & \quad + 4K^2 \lambda \gamma_t \delta_t + \frac{\gamma_t^2}{2} \sum_{k=1}^K \|\mathbf{V}_{k,t}\|_*^2 \end{aligned} \quad (\text{C.7})$$

holds for $\mathbf{Q}^ \in \mathcal{Q}^*$, where the sequence Z_t is defined as in (C.5).*

(ii) *With decreasing policy $(\gamma_t, \delta_t) = (\tilde{\gamma} t^{-\alpha}, \tilde{\delta} t^{-\beta})$, such that $\alpha, \beta \geq 0$ and $\tilde{\gamma}, \tilde{\delta} > 0$,*

$$\begin{aligned} R^* - \mathbb{E}[R(\bar{\mathbf{Q}}_t)] & \leq \frac{\mathcal{L}(\mathbf{Y}_1; \mathbf{Q}^*)}{\tilde{\gamma} \sum_{s=1}^t s^{-\alpha}} + \frac{4K^2 \lambda \tilde{\delta} \sum_{s=1}^t s^{-\alpha-\beta}}{\sum_{s=1}^t s^{-\alpha}} \\ & \quad + \frac{\tilde{\gamma} \sum_{s=1}^t s^{-2\alpha} \sum_{k=1}^K \|\mathbf{V}_{k,s}\|_*^2}{2 \sum_{s=1}^t s^{-\alpha}}. \end{aligned} \quad (\text{C.8})$$

(iii) *With constant policy $(\gamma_t, \delta_t) = (\tilde{\gamma}, \tilde{\delta})$, such that $\tilde{\gamma}, \tilde{\delta} > 0$,*

$$R^* - \mathbb{E}[R(\bar{\mathbf{Q}}_T)] \leq \frac{\mathcal{L}(\mathbf{Y}_1; \mathbf{Q}^*)}{T\tilde{\gamma}} + 4K^2 \lambda \tilde{\delta} + \frac{\tilde{\gamma} \sum_{t=1}^T \sum_{k=1}^K \|\mathbf{V}_{k,t}\|_*^2}{2T} \quad (\text{C.9})$$

for any $T \geq 1$. Further, if there exists $\bar{v} > 0$ such that $\|\mathbf{V}_{k,t}\|_ \leq \bar{v}$ for $k = 1, \dots, K$ and $t = 1, \dots, T$, then*

$$\mathbb{P}\left(\frac{1}{T\tilde{\gamma}} \sum_{t=1}^T Z_t \leq \varepsilon\right) \geq 1 - \exp\left(-\frac{T\varepsilon^2}{32\bar{v}^2 d^2}\right). \quad (\text{C.10})$$

Proof of Lemma C.1. (i) If $\mathbf{Q}^* \in \mathcal{Q}^*$, the concavity of R gives

$$\sum_{k=1}^K \langle \nabla_k R(\mathbf{Q}), \mathbf{Q}_k - \mathbf{Q}_k^* \rangle \leq R(\mathbf{Q}) - R^*, \quad \forall \mathbf{Q} \in \mathcal{Q}. \quad (\text{C.11})$$

It follows from Lemma A.2 that

$$\begin{aligned} \mathcal{L}(\mathbf{Y}_{t+1}; \mathbf{Q}^*) & \stackrel{(\text{MXL})}{=} \sum_{k=1}^K F(\mathbf{Q}_k^*, \mathbf{Y}_{k,t} + \gamma_t \mathbf{V}_{k,t}) \\ & \stackrel{(\text{A.11a})}{\leq} \mathcal{L}(\mathbf{Y}_t; \mathbf{Q}^*) + \sum_{k=1}^K \left[\gamma_t \langle \mathbf{V}_{k,t}, \mathbf{Q}_{k,t} - \mathbf{Q}_k^* \rangle + \frac{\gamma_t^2}{2} \|\mathbf{V}_{k,t}\|_*^2 \right] \\ & \stackrel{(\text{C.2})}{=} \mathcal{L}(\mathbf{Y}_t; \mathbf{Q}^*) + \gamma_t \sum_{k=1}^K \langle \nabla_k R(\mathbf{Q}_t), \mathbf{Q}_{k,t} - \mathbf{Q}_k^* \rangle + Z_t \\ & \quad + \sum_{k=1}^K \left[\gamma_t \langle \mathbf{B}_{k,t}, \mathbf{Q}_{k,t} - \mathbf{Q}_k^* \rangle + \frac{\gamma_t^2}{2} \|\mathbf{V}_{k,t}\|_*^2 \right], \end{aligned} \quad (\text{C.12})$$

Besides, (C.3) gives $|\langle \mathbf{B}_{k,t}, \mathbf{Q}_{k,t} - \mathbf{Q}_k^* \rangle| \leq 4K\lambda_k \delta_t$, which combined with (C.11) and (C.12) yields Inequality (C.7).

(ii) By telescoping (C.7) $t-1$ times, dividing by $\sum_{s=1}^t \gamma_s$, and using $\mathcal{L}(\mathbf{Y}_{n+1}; \mathbf{Q}^*) \geq 0$, we find

$$\begin{aligned} R^* - \frac{\sum_{s=1}^t \gamma_s R(\mathbf{Q}_s)}{\sum_{s=1}^t \gamma_s} & \leq \frac{\mathcal{L}(\mathbf{Y}_1; \mathbf{Q}^*)}{\sum_{s=1}^t \gamma_s} + \frac{\sum_{s=1}^t Z_s}{\sum_{s=1}^t \gamma_s} \\ & \quad + 4K^2 \lambda \frac{\sum_{s=1}^t \gamma_s \delta_s}{\sum_{s=1}^t \gamma_s} + \frac{1}{2} \frac{\sum_{s=1}^t \gamma_s^2 \sum_{k=1}^K \|\mathbf{V}_{k,s}\|_*^2}{\sum_{s=1}^t \gamma_s}. \end{aligned} \quad (\text{C.13})$$

By concavity of R , the time average of the estimates satisfies

$$R(\bar{\mathbf{Q}}_t) \geq \left(\frac{1}{\sum_{s=1}^t \gamma_s}\right) \sum_{s=1}^t \gamma_s R(\mathbf{Q}_s). \quad (\text{C.14})$$

Introducing the suggested policies in (C.13) and using (C.14) gives

$$\begin{aligned} R^* - R(\bar{\mathbf{Q}}_t) & \leq \frac{\mathcal{L}(\mathbf{Y}_1; \mathbf{Q}^*)}{\tilde{\gamma} \sum_{s=1}^t s^{-\alpha}} + \frac{\sum_{s=1}^t Z_s}{\tilde{\gamma} \sum_{s=1}^t s^{-\alpha}} \\ & \quad + 4K^2 \lambda \frac{\tilde{\delta} \sum_{s=1}^t s^{-\alpha-\beta}}{\sum_{s=1}^t s^{-\alpha}} + \frac{\tilde{\gamma} \sum_{s=1}^t s^{-2\alpha} \sum_{k=1}^K \|\mathbf{V}_{k,s}\|_*^2}{2 \sum_{s=1}^t s^{-\alpha}}. \end{aligned} \quad (\text{C.15})$$

Since (C.6a) lends $\{Z_t\}$ the quality of a martingale difference sequence, $\mathbb{E}[\sum_{s=1}^t Z_s] = 0$, and (C.8) follows by expectation of (C.15).

(iii) Setting $\alpha = \beta = 0$ in (C.8) gives us (C.9). By using the bounds $\bar{v}_1, \dots, \bar{v}_K$ in combination with (C.4) and (C.6b), we find that $|Z_t| \leq 4\bar{v}d\tilde{\gamma}$ for $t = 1, \dots, T$, and the martingale difference sequence $\{Z_t\}$ is bounded. It follows from Azuma's inequality that $\mathbb{P}(\sum_{t=1}^T Z_t > T\varepsilon\tilde{\gamma}) \leq \exp[-\frac{(T\tilde{\gamma}\varepsilon)^2}{2T(4\bar{v}d\tilde{\gamma})^2}]$ for any $\varepsilon > 0$, which is equivalent to (C.10). ■

Theorems 1 and 2 follow from Lemmas B.1 and C.1.

Proof of Theorem 1. Following the line of thought of the proof of [34, Theorem 5.1], we first show there one can find a solution $\mathbf{Q}^* \in \mathcal{Q}^*$ such that

$$\liminf_{t \rightarrow \infty} \mathcal{L}(\mathbf{Y}_t; \mathbf{Q}^*) = 0 \quad \text{a.s.} \quad (\text{C.16})$$

Next, we see that $\{\mathcal{L}(\mathbf{Y}_t; \mathbf{Q}^*)\}$ converges almost surely (a.s.) towards a finite quantity which, in view of (C.16), can only be 0. A.s. convergence of $\{\mathbf{Q}_t\}$ towards \mathbf{Q}^* can then be inferred from Lemma A.2-(A.11b). The assumption of non-increasing $\{\delta_t\}$, together with (20a) and (20b), implies $\delta_t \downarrow 0$ which, in view of (B.3), secures a.s. convergence of $\{\hat{\mathbf{Q}}_t\}$ as well.

First observe that (C.16) holds if, almost surely, there exists a subsequence of $\{\mathbf{Q}_t\}$ that converges towards a solution $\mathbf{Q}^* \in \mathcal{Q}^*$. Suppose this condition not to hold, and let \mathcal{S} denote the set of the limit points of all subsequences of $\{\mathbf{Q}_t\}$. Then, almost surely, we have $\mathcal{Q}^* \cap \mathcal{S} = \emptyset$ and, since \mathcal{S} is closed by construction and R is continuous and convex, $\varrho := R^* - \max_{\mathbf{Q} \in \mathcal{S}} R(\mathbf{Q}) > 0$.

Telescoping (C.7) in Lemma C.1(i) and using (B.5), yields

$$\begin{aligned} \mathcal{L}(\mathbf{Y}_{t+1}; \mathbf{Q}^*) &\leq \mathcal{L}(\mathbf{Y}_1; \mathbf{Q}^*) - \sum_{s=1}^t \gamma_s [R^* - R(\mathbf{Q}_s)] \\ &\quad + \sum_{s=1}^t Z_s + 4K^2\lambda \sum_{s=1}^t \gamma_s \delta_s + \frac{K(R^*d)^2}{2^{2K+1}} \sum_{s=1}^t \frac{\gamma_s^2}{\delta_s^2}, \end{aligned} \quad (\text{C.17})$$

where $\{Z_t\}$ is the difference sequence of a martingale with respect to the filtration $\{\mathcal{F}_t\}$. In view of (20b) and (20c), the last two terms in the second member of (C.17) converge as $t \rightarrow \infty$. As for the third term, since

$$\sum_{s=1}^{\infty} \mathbb{E}[Z_s^2 | \mathcal{F}_{s-1}] \leq \frac{4K(R^*d)^2}{2^{2K}} \sum_{s=1}^{\infty} \frac{\gamma_s^2}{\delta_s^2} \stackrel{(20c)}{<} \infty, \quad (\text{C.18})$$

[35, Theorem 2.18] applies with parameter $p = 2$, and it follows that $\sum_{s=1}^t Z_s$ converges a.s. as $t \rightarrow \infty$. Finally, one can find a subsequence $\{\mathbf{Q}_{t_s}\}$ that converges to a point of \mathcal{S} and thus satisfies $R^* - R(\mathbf{Q}_{t_s}) > \varrho/2$ for s large enough. It follows from (20a) that the second term $\sum_{s=1}^{\infty} \gamma_s [R(\mathbf{Q}_t) - R(\mathbf{Q}^*)] \rightarrow -\infty$. All in all we find that $\mathcal{L}(\mathbf{Y}_t; \mathbf{Q}^*) \rightarrow -\infty$ a.s., which is in contradiction with the nonnegativity of \mathcal{L} . We infer that (C.16) is true.

It remains to show that $\{\mathcal{L}(\mathbf{Y}_t; \mathbf{Q}^*)\}$ is almost surely convergent. To do so we rely on Doob's convergence theorem for supermartingales [35, Theorem 2.5]. Recalling (C.7), and using (B.5) and $R(\mathbf{Q}_t) - R(\mathbf{Q}^*) \leq 0$, we find

$$\mathcal{L}(\mathbf{Y}_{t+1}; \mathbf{Q}^*) \leq \mathcal{L}(\mathbf{Y}_t; \mathbf{Q}^*) + Z_t + 4K^2\lambda\gamma_t\delta_t + \frac{K(R^*d\gamma_t)^2}{2^{2K+1}\delta_t^2}. \quad (\text{C.19})$$

Consider $S_t = \sum_{s=t+1}^{\infty} [4K^2\lambda\gamma_s\delta_s + K(R^*d\gamma_s)^2/(2^{2K+1}\delta_s^2)] + \mathcal{L}(\mathbf{Y}_{t+1}; \mathbf{Q}^*)$. Under assumptions (20b) and (20c), S_0 is finite by construction. We infer from (C.6a) and (C.19) that $\mathbb{E}[S_t | \mathcal{F}_{t-1}] \leq S_{t-1}$ for $t \geq 1$, and $\{S_t\}$ is a supermartingale with respect to $\{\mathcal{F}_t\}$, thus satisfying $\mathbb{E}[S_t] \leq S_0 < \infty$. Hence, $\{S_t\}$ is uniformly L^1 -bounded and Doob's theorem applies. It follows that $\{S_t\}$, and

consequently $\{\mathcal{L}(\mathbf{Y}_t; \mathbf{Q}^*)\}$, are almost surely convergent, which completes the proof. ■

Proof of Theorem 2. By considering Lemma C.1(iii) with the upper bounds $(d\bar{v}) = dR^*/(2^{K-1}\tilde{\delta})$ supplied by (B.5), we find

$$R^* - \mathbb{E}[R(\hat{\mathbf{Q}}_T)] \stackrel{(C.9)}{\leq} \frac{K \log M}{T\tilde{\gamma}} + 4K^2\lambda\tilde{\delta} + \frac{K(R^*d)^2\tilde{\gamma}}{2^{2K-1}\tilde{\delta}^2}, \quad (\text{C.20})$$

where we have used $\mathcal{L}(\mathbf{Y}_1; \mathbf{Q}^*) \leq K \log M$, and

$$\mathbb{P}(\frac{1}{T\tilde{\gamma}} \sum_{t=1}^T Z_t \leq \varepsilon) \stackrel{(C.10)}{\geq} 1 - \exp(-\frac{2^{2K-5}T\varepsilon^2\tilde{\delta}^2}{(R^*Kd)^2}). \quad (\text{C.21})$$

The right member of (C.20) is convex in $(\tilde{\gamma}, \tilde{\delta})$ and minimized for the policy $(\tilde{\gamma}, \tilde{\delta}) = (\gamma T^{-3/4}, \delta T^{-1/4})$, where

$$\gamma = \sqrt{\frac{2^K}{\lambda R^* K d}} \left(\frac{\log M}{2}\right)^{3/4}, \quad \delta = 2 \sqrt{\frac{\lambda R^* K^3 d}{2^K}} \left(\frac{\log M}{2}\right)^{1/4}. \quad (\text{C.22})$$

Less specifically, we find (27) by substituting $\tilde{\gamma}$ and $\tilde{\delta}$ in (C.20) with the suggestion $(\tilde{\gamma}, \tilde{\delta}) = (\gamma T^{-3/4}, \delta T^{-1/4})$. Then, (28) follows from (27) and (C.21) after setting $\tilde{\delta} = \delta T^{-1/4}$ in the right member of (C.21). Claims (a) and (b) have been shown. ■

D. Analysis of the MXL0⁺ algorithm

The $\mathcal{O}(\delta)$ bound for the bias in Lemma B.1 still holds when the SPSAplus gradient estimator is used. The offset in (SPSA+) allows us, however, to derive an $\mathcal{O}(1/\delta)$ bound for the norm, in place of the harmful $\mathcal{O}(1/\delta)$ bound inherent with SPSA.

Lemma D.1. *If MXL0⁺ is implemented under (H0) and (H3)-(H4), then $\|\mathbf{V}_{k,t}\|_*$ is uniformly bounded for $k = 1, \dots, K$.*

In particular, if $(\gamma_t, \delta_t) = (\gamma t^{-\alpha}, \delta t^{-\beta})$ with

$$(a) \quad 0 \leq \beta \leq \alpha, \quad (b) \quad dLK\gamma < 2\delta, \quad (\text{D.1})$$

then there is $\bar{v}_{\alpha,\beta}(\gamma, \delta) < \infty$ such that $\|\mathbf{V}_{k,t}\|_ \leq \frac{d_k}{2} \bar{v}_{\alpha,\beta}(\gamma, \delta)$ holds for all t and for $k = 1, \dots, K$ and, when $\beta = 0$,*

$$\bar{v}_{\alpha,0}(\gamma, \delta) = \left(\frac{4\tau_{\alpha}}{\sqrt{d}}\right) \left(\frac{2}{dLK} - \frac{\gamma}{\delta}\right)^{-1}. \quad (\text{D.2})$$

Proof of Lemma D.1. With the convention $\rho_0 = R(\mathbf{Q}_1)$, we have, for $k = 1, \dots, K$,

$$\begin{aligned} \|\mathbf{V}_{k,1}\|_* &\stackrel{(\text{SPSA}^+)}{\leq} \frac{d_k}{\delta_1} |R(\hat{\mathbf{Q}}_1) - R(\mathbf{Q}_1)| \|\mathbf{Z}_{k,1}\|_* \\ &\stackrel{(10)}{\leq} \frac{d_k L}{2\delta_1} \|\hat{\mathbf{Q}}_1 - \mathbf{Q}_1\| \stackrel{(\text{B.3})}{\leq} d_k LK \sqrt{d}, \end{aligned} \quad (\text{D.3})$$

and it follows from (A.2) that $\|\mathbf{V}_1\|_* \leq dLK \sqrt{d}$. For $t \geq 2$,

$$\begin{aligned} \|\mathbf{V}_{k,t}\|_* &\stackrel{(\text{SPSA}^+)}{\leq} \frac{d_k}{\delta_t} |R(\hat{\mathbf{Q}}_t) - R(\hat{\mathbf{Q}}_{t-1})| \|\mathbf{Z}_{k,t}\|_* \\ &\leq \frac{d_k}{2\delta_t} [|R(\hat{\mathbf{Q}}_t) - R(\mathbf{Q}_t)| + |R(\mathbf{Q}_t) - R(\mathbf{Q}_{t-1})| \\ &\quad + |R(\hat{\mathbf{Q}}_{t-1}) - R(\mathbf{Q}_{t-1})|] \\ &\stackrel{(10)}{\leq} \frac{d_k}{2\delta_t} [L\|\hat{\mathbf{Q}}_t - \mathbf{Q}_t\| + L\|\mathbf{Q}_t - \mathbf{Q}_{t-1}\| \\ &\quad + L\|\hat{\mathbf{Q}}_{t-1} - \mathbf{Q}_{t-1}\|] \\ &\stackrel{(\text{B.3})}{\leq} \frac{d_k L}{2\delta_t} [2K \sqrt{d}(\delta_t + \delta_{t-1}) + \sum_{k=1}^K \|\mathbf{Q}_{k,t} - \mathbf{Q}_{k,t-1}\|] \\ &\stackrel{(\text{A.9})}{\leq} \frac{d_k L}{2\delta_t} [2K \sqrt{d}(\delta_t + \delta_{t-1}) + K\gamma_t \|\mathbf{V}_{t-1}\|_*], \end{aligned} \quad (\text{D.4})$$

so that $\|\mathbf{V}_t\|_* \leq \frac{dL}{2\delta_t} [2K \sqrt{d}(\delta_t + \delta_{t-1}) + K\gamma_t \|\mathbf{V}_{t-1}\|_*]$. With the convention $\delta_0 = 0$, we find, by induction on t ,

$$\|\mathbf{V}_{k,t}\|_* \leq LKd_k \sqrt{d} \sum_{s=1}^t \left(\frac{dLK}{2}\right)^{t-s} \prod_{u=s+1}^t \frac{\gamma_{u-1}}{\delta_{u-1}} \left(1 + \frac{\delta_{s-1}}{\delta_s}\right). \quad (\text{D.5})$$

Condition (H4) tells us that δ_{t-1}/δ_t is uniformly bounded by a finite constant, say, $c < \infty$, while (H3) rewrites as

$$q := \frac{dLK}{2} \left(\sup_{t \geq 2} \frac{\gamma_{t-1}}{\delta_t} \right) < 1. \quad (\text{D.6})$$

Using $\frac{\gamma_{t-1}}{\delta_t} \leq \frac{2q}{dLK}$ and $\frac{\delta_{t-1}}{\delta_t} \leq c$ in (D.5), we find, for $t \geq 2$,

$$\frac{\|\mathbf{V}_{k,t}\|_*}{LKd_k \sqrt{d}} \leq \sum_{s=1}^t q^{t-s} (1+c) = (1+c) \frac{1-q^t}{1-q} \leq \frac{1+c}{1-q}. \quad (\text{D.7})$$

Under the policies $\gamma_t = \gamma t^{-\alpha}$ and $\delta_t = \delta t^{-\beta}$, (D.5) becomes

$$\|\mathbf{V}_{k,t}\|_* \leq \tau_\alpha d_k LK \sqrt{d} \sum_{s=1}^t \left(\frac{\gamma d LK}{2\delta} \right)^{t-s} \left(\frac{t}{s} \right)^\beta \left[\frac{(t-1)!}{(s-1)!} \right]^{\beta-\alpha}, \quad (\text{D.8})$$

where $\tau_\alpha = 1 + 2^\alpha$. Under Condition (D.1a) the last factor is no larger than 1, and we obtain the uniform bound with

$$\bar{v}_{\alpha,\beta}(\gamma, \delta) = 2L(1 + 2^\alpha)K \sqrt{d} \sum_{s=1}^\infty \left[\frac{\gamma d LK}{2\delta} \right]^{t-s} \left(\frac{t}{s} \right)^\beta, \quad (\text{D.9})$$

which is finite on condition that (D.1b) holds. For $\beta = 0$, (D.9) reduces to a geometric series and (D.2) follows directly. ■

We are now able to show Theorem 3 and Theorem 4. Again, the Lyapunov function (C.1) and Lemma C.1 are used.

Proof of Theorem 3. Proceed as in the proof of Theorem 1, now with assumptions (H1a), (H1b) and (H2) in place of (20a), (20b), (20c). Because the conditions of Lemma D.1 are met, there exists $\bar{v} < \infty$ such that $\|\mathbf{V}_{k,t}\|_* < \bar{v}$ for all k , so that (C.17) and (C.19) respectively become, for some $\mathbf{Q}^* \in \mathcal{Q}^*$,

$$\begin{aligned} \mathcal{L}(\mathbf{Y}_{t+1}; \mathbf{Q}^*) &\leq \mathcal{L}(\mathbf{Y}_t; \mathbf{Q}^*) - \sum_{s=1}^t \gamma_s [R^* - R(\mathbf{Q}_s)] \\ &\quad + \sum_{s=1}^t Z_s + 4K^2 \lambda \sum_{s=1}^t \gamma_s \delta_s + \frac{K\bar{v}^2}{2} \sum_{s=1}^t \gamma_s^2, \end{aligned} \quad (\text{D.10})$$

with $\sum_{s=1}^\infty \mathbb{E} \left[Z_s^2 | \mathcal{F}_{s-1} \right] \leq (4K\bar{v})^2 \sum_{s=1}^\infty \gamma_s^2 < \infty$, and

$$\mathcal{L}(\mathbf{Y}_{t+1}; \mathbf{Q}^*) \leq \mathcal{L}(\mathbf{Y}_t; \mathbf{Q}^*) + Z_t + 4K^2 \lambda \gamma_t \delta_t + \frac{K\bar{v}^2}{2} \gamma_t^2. \quad (\text{D.11})$$

Thus, $S_t = \mathcal{L}(\mathbf{Y}_{t+1}; \mathbf{Q}^*) + \sum_{s=t+1}^\infty [4K^2 \lambda \gamma_s \delta_s + K\bar{v}^2 \gamma_s^2 / 2]$ now defines the supermartingale with respect to $\{\mathcal{F}_t\}$. ■

Proof of Theorem 4. (1) By combining the uniform bound in Lemma D.1 with (C.8) in Lemma C.1(ii) and using $\mathcal{L}(\mathbf{Y}_1; \mathbf{Q}^*) \leq K \log M$, we find, for the policy $(\gamma_t, \delta_t) = (\tilde{\gamma} t^{-\alpha}, \tilde{\delta} t^{-\beta})$,

$$\begin{aligned} R^* - \mathbb{E}[R(\bar{\mathbf{Q}}_t)] &\leq \frac{K \log M}{\gamma \sum_{s=1}^t s^{-\alpha}} + 4K^2 \lambda \delta \frac{\sum_{s=1}^t s^{-\alpha-\beta}}{\sum_{s=1}^t s^{-\alpha}} \\ &\quad + \frac{Kd^2 [\bar{v}_{\alpha,\beta}(\gamma, \delta)]^2 \gamma \sum_{s=1}^t s^{-2\alpha}}{8 \sum_{s=1}^t s^{-\alpha}}, \end{aligned} \quad (\text{D.12})$$

where $\bar{v}_{\alpha,\beta}(\gamma, \delta)$ is given by (D.9). The above upper bound is minimized for $\alpha = \beta = 1/2$, in which case we find (26).

(2) Using Lemma C.1(iii) under $(\tilde{\gamma}, \tilde{\delta}) = (\gamma / \sqrt{T}, \delta / \sqrt{T})$ and with the bounds $\bar{v} = \frac{1}{2} \bar{v}_{0,0}(\tilde{\gamma}, \tilde{\delta})$, given by Lemma D.1, yields

$$R^* - \mathbb{E}[R(\bar{\mathbf{Q}}_T)] \stackrel{(\text{C.9})}{\leq} \frac{K \log M}{\gamma \sqrt{T}} + \frac{4K^2 \lambda \delta}{\sqrt{T}} + \frac{Kd^2 [\bar{v}_{0,0}(\frac{\gamma}{\sqrt{T}}, \frac{\delta}{\sqrt{T}})]^2 \gamma}{8 \sqrt{T}} \quad (\text{D.13})$$

where $\bar{v}_{0,0}(\tilde{\gamma}, \tilde{\delta}) = \left(\frac{8}{\sqrt{d}} \right) \left(\frac{2}{dLK} - \frac{\gamma}{\delta} \right)^{-1}$, and

$$\mathbb{P} \left(\frac{\sum_{t=1}^T Z_t}{\sqrt{T} \gamma} \leq \varepsilon \right) \stackrel{(\text{C.10})}{\geq} 1 - \exp \left(- \frac{T \varepsilon^2}{8K^2 d^2 [\bar{v}_{0,0}(\frac{\gamma}{\sqrt{T}}, \frac{\delta}{\sqrt{T}})]^2} \right). \quad (\text{D.14})$$

We find (21) after substituting $\bar{v}_{0,0}(\tilde{\gamma}, \tilde{\delta})$ with its actual value in (D.13). Then, (22) follows from (21) and (D.14). ■

The proof of Corollary 1 relies on the following lemma.

Lemma D.2. Let $\Gamma = \{(\gamma, \delta) \in \mathbb{R}_{>0} \times \mathbb{R}_{>0} : \gamma < h\delta\}$ and consider the function $f : \Gamma \mapsto \mathbb{R}$ defined by

$$f(\gamma, \delta) = \frac{a}{\gamma} + 2b\delta + c\gamma \left(h - \frac{\gamma}{\delta} \right)^{-2} + d \left(h - \frac{\gamma}{\delta} \right)^{-1}, \quad (\text{D.15})$$

where $a, b, c, h > 0$ and $d \geq 0$ are given parameters.

(i) At the point $(\gamma^*, \delta^*) \in \Gamma$, where

$$\gamma^* = h \left[\sqrt{\frac{c}{a}} + \sqrt{\sqrt{\frac{c}{a}} \left(\frac{2bh}{2\sqrt{ac+d}} \right)} \right]^{-1}, \quad \delta^* = \sqrt{\sqrt{\frac{a}{c}} \left(\frac{2\sqrt{ac+d}}{2bh} \right)}, \quad (\text{D.16})$$

the value of f is given by

$$f(\gamma^*, \delta^*) = \frac{2\sqrt{ac+d}}{h} + 2\sqrt{2b\sqrt{\frac{a}{c}} \left(\frac{2\sqrt{ac+d}}{h} \right)}. \quad (\text{D.17})$$

Under the constraint $\delta / \sqrt{t} < r$, where $r > 0$, (D.17) holds for

$$t > \sqrt{\frac{a}{c}} \left(\frac{2\sqrt{ac+d}}{2bh} \right) r^{-2}. \quad (\text{D.18})$$

(ii) For any $\varepsilon > 0$, $f(\gamma^*, \delta^*) / \sqrt{t} \leq \varepsilon$ holds for $t \geq T$ if $T = \lceil f(\gamma^*, \delta^*) / \varepsilon^2 \rceil$. The constraint $\delta^* / \sqrt{T} < r$ then rewrites as

$$\varepsilon < \left(4b + \sqrt{2(b/h)\sqrt{c/a}(2\sqrt{ac+d})} \right) r. \quad (\text{D.19})$$

Proof. Verification of all the claims is straightforward. ■

Proof of Corollary 1. (a) To derive γ and δ in (a) it suffices to apply Lemma D.2(i) to the expression for $B(\gamma, \delta)$ given in Theorem 4(2a). The convergence rate of $\mathbb{E}[R(\bar{\mathbf{Q}}_T)]$ follows from (27) and (D.17), while the condition on T is a translation of (D.18) into the present setting, where the restriction $\delta / \sqrt{s} < r_k$ for all k applies, with r_k given by (19).

(b) Recall Theorem 4(2b). The second member of (28) rewrites as $1 - \alpha$ on condition that we set

$$\varepsilon = 16 \left[\frac{2}{LK(M^2-1)} - \frac{\gamma}{\delta} \right]^{-1} \sqrt{\frac{2 \log(\frac{1}{\alpha}) K^2 (M^2-1)}{T}}.$$

Observe that $B(\gamma, \delta) + \varepsilon \sqrt{T}$ is an instance of the function $f(\gamma, \delta)$ defined in (D.15). Lemma D.2(ii) gives us a condition on T for $B(\gamma, \delta) / \sqrt{T} + \varepsilon \leq \varepsilon$ to be true which, in view of (28), is also sufficient for (30) to hold. After computations we find the value of T in Table Ib with the restriction on ε :

$$\varepsilon \stackrel{(\text{D.19})}{\leq} 2^{\frac{9}{4}} \lambda \left[\phi(\alpha) \sqrt{\frac{L}{\lambda}} + \frac{2^{\frac{3}{4}}}{\sqrt[4]{\log(\frac{1}{\alpha}) [M^2-1]}} \right] \sqrt{\frac{\sqrt{\log(\frac{1}{\alpha})} K^4 [M+1] [M^2-1]}{M}}. \quad (\text{D.20})$$

E. Analysis of the AMXL0⁺ algorithm

Lemmas B.1 and D.1 still apply in the asynchronous setting. Instead of (C.1) we use the Lyapunov function

$$\mathcal{L}_\pi(\mathbf{Y}; \mathbf{Q}^*) = \sum_{k=1}^K \frac{1}{\pi_k} F(\mathbf{Q}_k^*, \mathbf{Y}_k), \quad (\text{E.1})$$

where $\mathbf{Q}^* \in \mathcal{Q}^*$ is a solution. Proceeding as for the derivation of (C.12) in Lemma C.1, we find, for the algorithm (AMXL0⁺),

$$\begin{aligned} \mathcal{L}_\pi(\mathbf{Y}_{t+1}; \mathbf{Q}^*) &\leq \mathcal{L}_\pi(\mathbf{Y}_t; \mathbf{Q}^*) - \gamma_t [R^* - R(\mathbf{Q}_t)] \\ &\quad + 4K^2 \lambda \gamma_t \delta_t + X_t + \sum_{k=1}^K \frac{\gamma_t^2}{2} \|\mathbf{V}_{k,t}\|_*^2, \end{aligned} \quad (\text{E.2})$$

with the random sequence $\{X_t\}$ now given by

$$\begin{aligned} X_t &= \gamma_t \sum_{k \in U_t} \langle \mathbf{U}_{k,t}, \mathbf{Q}_{k,t} - \mathbf{Q}_k^* \rangle \\ &\quad + \sum_{k=1}^K \frac{1_{U_t}(k) - \pi_k}{\pi_k} [\gamma_t \langle \mathbf{V}_{k,t}, \mathbf{Q}_{k,t} - \mathbf{Q}_k^* \rangle + \frac{\gamma_t^2}{2} \|\mathbf{V}_{k,t}\|_*^2], \end{aligned} \quad (\text{E.3})$$

where we used the indicator function: $\mathbf{1}_{U_t}(k) = 1$ if $k \in U_t$, and $\mathbf{1}_{U_t}(k) = 0$ otherwise. It is easily seen that $\mathbb{E}[X_t | \mathcal{F}_{t-1}] = 0$, and

$$|X_t| \leq 2\gamma_t \sum_{k=1}^K \|\mathbf{U}_{k,t}\|_* + \sum_{k=1}^K \max\left(1, \frac{1}{\pi_k} - 1\right) \left[2\gamma_t \|\mathbf{V}_{k,t}\|_* + \frac{\gamma_t^2}{2} \|\mathbf{V}_{k,t}\|_*^2\right]. \quad (\text{E.4})$$

Compare (E.2),(E.4) with (C.7),(C.6b). By reproducing the rationale behind the proof of Lemma C.1, we obtain an asynchronous counterpart to Lemma C.1, where (C.8) and (C.9) now hold with \mathcal{L}_π in place of \mathcal{L} , and (C.10) becomes

$$\mathbb{P}\left(\frac{\sum_{t=1}^T X_t}{T\bar{\gamma}} \geq \zeta\right) \leq \exp\left(-\frac{T\zeta^2}{8K^2 d^2 \left[\left(1 + \frac{\nu_\pi}{2}\right)\bar{v}_{0,0}(\bar{\gamma}, \bar{\delta}) + \frac{\nu_\pi}{8}\bar{\gamma}d \left[\bar{v}_{0,0}(\bar{\gamma}, \bar{\delta})\right]^2\right]}\right), \quad (\text{E.5})$$

where ν_π is defined as in Theorem 5.

Proof of Theorem 5. Proceed as in the proof of Theorem 4 with the above observations in mind. ■

Proof of Corollary 2. First observe that we have $\nu_\pi = K - 1$ if $K \geq 2$. The rest of the proof bases on the conclusions of Theorem 5 and follows the exact lines of the proof of Corollary 1, now using $B_\pi(\gamma, \delta)$ and $C_\pi(\gamma, \delta)$. Note that Corollary 2b holds with the following restriction on ε :

$$\varepsilon \stackrel{(\text{D.19})}{<} 2^3 \lambda \left[\hat{\phi}_\pi(\alpha) \sqrt{\frac{\hat{\chi}(\alpha)L}{\lambda}} + \left[\log^{\frac{3}{8}}(1/\alpha) K^{\frac{3}{4}} d \right]^{-1} \sqrt{\frac{\log^{\frac{3}{4}}(\frac{1}{\alpha}) K^{\frac{1}{4}} \frac{1}{M+1} \lfloor M^2 - 1 \rfloor}{M}} \right]. \quad (\text{E.6})$$

[13] —, “Simultaneous iterative water-filling for Gaussian frequency-selective interference channels,” in *ISIT '06: Proceedings of the 2006 International Symposium on Information Theory*, 2006.

[14] P. Mertikopoulos and A. L. Moustakas, “Learning in an uncertain world: MIMO covariance matrix optimization with imperfect feedback,” *IEEE Trans. Signal Process.*, vol. 64, no. 1, pp. 5–18, January 2016.

[15] R. Liao, B. Bellalta, M. Oliver, and Z. Niu, “MU-MIMO MAC protocols for wireless local area networks: A survey,” *IEEE Commun. Surveys Tuts.*, vol. 18, no. 1, pp. 162–183, January 2016.

[16] J. C. Spall, “A one-measurement form of simultaneous perturbation stochastic approximation,” *Automatica*, vol. 33, no. 1, pp. 109–112, 1997.

[17] A. D. Flaxman, A. T. Kalai, and H. B. McMahan, “Online convex optimization in the bandit setting: gradient descent without a gradient,” in *SODA '05: Proceedings of the 16th annual ACM-SIAM Symposium on Discrete Algorithms*, 2005, pp. 385–394.

[18] W. Li and M. Assaad, “Matrix exponential learning schemes with low informational exchange,” *IEEE Trans. Signal Process.*, vol. 67, no. 12, pp. 3140–3153, April 2019.

[19] I. E. Telatar, “Capacity of multi-antenna Gaussian channels,” *European Transactions on Telecommunications and Related Technologies*, vol. 10, no. 6, pp. 585–596, 1999.

[20] D. Monderer and L. S. Shapley, “Potential games,” *Games and Economic Behavior*, vol. 14, no. 1, pp. 124–143, 1996.

[21] A. Neyman, “Correlated equilibrium and potential games,” *International Journal of Game Theory*, vol. 26, no. 2, pp. 223–227, June 1997.

[22] G. Scutari, D. P. Palomar, and S. Barbarossa, “The MIMO iterative waterfilling algorithm,” *IEEE Trans. Signal Process.*, vol. 57, no. 5, pp. 1917–1935, May 2009.

[23] Z.-Q. Luo and J.-S. Pang, “Analysis of iterative waterfilling algorithms for multi-user power control in digital subscriber lines,” *EURASIP J. Appl. Signal Process. [Online]*, May 2006.

[24] P. Mertikopoulos, E. V. Belmega, A. L. Moustakas, and S. Lasaulce, “Distributed learning policies for power allocation in multiple access channels,” *IEEE J. Sel. Areas Commun.*, vol. 30, no. 1, pp. 96–106, January 2012.

[25] P. Mertikopoulos, E. V. Belmega, and A. L. Moustakas, “Matrix exponential learning: Distributed optimization in MIMO systems,” in *ISIT '12: Proceedings of the 2012 IEEE International Symposium on Information Theory*, 2012, pp. 3028–3032.

[26] Y. Nesterov, “Primal-dual subgradient methods for convex problems,” *Mathematical Programming*, vol. 120, no. 1, pp. 221–259, 2009.

[27] Y.-L. Yu, “The strong convexity of von Neumann’s entropy,” June 2013, unpublished note. [Online]. Available: <http://www.cs.cmu.edu/~yaoliang/mynotes/sc.pdf>

[28] A. Shapiro, D. Dentcheva, and A. Ruszczyński, *Lectures on stochastic programming: modeling and theory*, ser. MPS-SIAM series on optimization. Philadelphia: Society for Industrial and Applied Mathematics, 2009.

[29] J. Hiriart-Urruty and C. Lemaréchal, *Fundamentals of Convex Analysis*, ser. Grundlehren Text Editions. Springer Berlin Heidelberg, 2004.

[30] R. T. Rockafellar, *Convex analysis*, ser. Princeton Mathematical Series. Princeton, N. J.: Princeton University Press, 1970.

[31] S. M. Kakade, S. Shalev-Shwartz, and A. Tewari, “Regularization techniques for learning with matrices,” *J. Mach. Learn. Res.*, vol. 13, pp. 1865–1890, Jun. 2012. [Online]. Available: <http://dl.acm.org/citation.cfm?id=2188385.2343703>

[32] Y. Nesterov, *Introductory Lectures on Convex Optimization: A Basic Course*, 1st ed. Springer Publishing Company, Incorporated, 2014.

[33] M. Bravo, D. S. Leslie, and P. Mertikopoulos, “Bandit learning in concave N -person games,” in *NIPS '18: Proceedings of the 32nd International Conference on Neural Information Processing Systems*, 2018.

[34] —, “Bandit learning in concave n -person games,” 2018.

[35] P. Hall and C. C. Heyde, *Martingale limit theory and its application / P. Hall, C.C. Heyde*. Academic Press New York, 1980.

REFERENCES

[1] E. G. Larsson, O. Edfors, F. Tufvesson, and T. L. Marzetta, “Massive MIMO for next generation wireless systems,” *IEEE Commun. Mag.*, vol. 52, no. 2, pp. 186–195, February 2014.

[2] J. G. Andrews, S. Buzzi, W. Choi, S. Hanly, A. Lozano, A. C. K. Soong, and J. C. Zhang, “What will 5G be?” *IEEE J. Sel. Areas Commun.*, vol. 32, no. 6, pp. 1065–1082, June 2014.

[3] J. S.-B. Orange, A. G. Armada, B. Evans, A. Galis, and H. Karl, “White paper for research beyond 5G,” *Accessed*, vol. 23, 2015.

[4] E. C. Strinati, S. Barbarossa, J. L. Gonzalez-Jimenez, D. Kténas, N. Cassiau, and C. Dehos, “6G: The next frontier,” *arXiv preprint arXiv:1901.03239*, 2019.

[5] J. Hoydis, S. ten Brink, and M. Debbah, “Massive MIMO in the UL/DL of cellular networks: How many antennas do we need?” *IEEE Trans. Wireless Commun.*, vol. 31, no. 2, pp. 160–171, February 2013.

[6] F. Rusek, D. Persson, B. K. Lau, E. G. Larsson, T. L. Marzetta, O. Edfors, and F. Tufvesson, “Scaling up MIMO: Opportunities and challenges with very large arrays,” *IEEE Signal Process. Mag.*, vol. 30, pp. 40–60, January 2013.

[7] R. S. Cheng and S. Verdú, “Gaussian multiaccess channels with ISI: capacity region and multiuser water-filling,” *IEEE Trans. Inf. Theory*, vol. 39, no. 3, pp. 773–785, May 1993.

[8] W. Yu, W. Rhee, S. Boyd, and J. M. Cioffi, “Iterative water-filling for Gaussian vector multiple-access channels,” *IEEE Trans. Inf. Theory*, vol. 50, no. 1, pp. 145–152, 2004.

[9] G. Scutari, D. P. Palomar, and S. Barbarossa, “Optimal linear precoding strategies for wideband non-cooperative systems based on game theory – part I: Nash equilibria,” *IEEE Trans. Signal Process.*, vol. 56, no. 3, pp. 1230–1249, March 2008.

[10] —, “Optimal linear precoding strategies for wideband non-cooperative systems based on game theory – part II: algorithms,” *IEEE Trans. Signal Process.*, vol. 56, no. 3, pp. 1250–1267, March 2008.

[11] E. V. Belmega, S. Lasaulce, M. Debbah, M. Jungers, and J. Dumont, “Power allocation games in wireless networks of multi-antenna terminals,” *Telecommunication Systems*, vol. 47, no. 1-2, pp. 109–122, 2011.

[12] G. Scutari, D. P. Palomar, and S. Barbarossa, “Asynchronous iterative water-filling for Gaussian frequency-selective interference channels,” *IEEE Trans. Inf. Theory*, vol. 54, no. 7, pp. 2868–2878, July 2008.